METEOR -Berichte

Coupled benthic and pelagic oxygen, nutrient and trace metal cycling, ventilation and carbon degradation in the oxygen minimum zone of the Peruvian continental margin (SFB 754).

Cruise No. M 136

11.04. – 03.05.2017

Callao (Peru) – Callao

Solute-Flux Peru I

Marcus Dengler, Stefan Sommer and the shipboard party

Chief Scientist Marcus Dengler

GEOMAR Helmholtz Centre for Ocean Research Kiel

2019

Table of contents

1 Cruise summary

1.1 Summary in English

The magnitude of nutrient and trace metal cycling in oxygen minimum zones (OMZ) and the involved loss of fixed nitrogen is crucial for the ocean's nutrient budget, particularly in light of the ongoing expansion of OMZs. The major focus of the measurement program that was carried out in the frame of the DFG Collaborative Research Centre (SFB) 754 „Climate-biogeochemical interactions in the tropical ocean", was to advance interdisciplinary understanding of benthic and pelagic nutrient and trace metal cycling processes in the OMZ off Peru and to quantify loss of nitrogen nutrients. Further objectives were to determine ventilation rates by submesoscale processes, quantify export fluxes of particulate organic matter, determine production and decay rates of dissolved organic material, and investigate mechanisms of iron stabilization, removal and cycling. The physical-biogeochemical measurement program focused on a transect perpendicular to the coastline at 12°S. Additionally, a transect at 14°S was completed and a submesoscale process study in an upwelling filament structure was carried out in the region of 15°S, 77°W. The coordinated sampling scheme included CTD profiling and water sampling stations, shipboard turbulence and velocity observations, a glider swarm experiment, moored velocity and hydrography observations, in situ benthic flux measurements using landers, sediment retrieval with a multiple corer, drifting sediment trap deployments and recovery and in situ pump deployments. The measurement program that was closely linked to the follow-up cruise M137 was successfully completed and all data sets were acquired as planned.

1.2 Zusammenfassung

Die Stärke der benthischen und pelagischen Umwandlungsprozesse von Nährstoffen und Spurenmetallen in Sauerstoffminimumzonen (SMZ) und der damit einhergehende Verlust von Stickstoffverbindungen ist für den Nährstoffhaushalt im Ozean von entscheidender Bedeutung, besonders im Hinblick auf die gegenwärtig beobachtete Ausbreitung von SMZ. Die Hauptzielsetzung des interdisziplinären Messprogramms, das im Rahmen des Kieler SFB 754 „Climate-biogeochemical interactions in the tropical ocean" durchgeführt wurde, war das benthisch pelagische Nährstoff- und Spurenmetallbudget quantitativ zu erfassen und die Verlustraten von Nährstoffen in der SMZ zu bestimmen. Weitere Zielsetzungen waren die Quantifizierung der Ventilationsraten durch submesoskalige Prozesse, die Bestimmung des Exports von partikulärem organischem Material und der Produktionsraten und des Abbaus von gelöstem organischem Material sowie Untersuchungen zu Stabilisierung, Regenerierung und dem Abbau von Eisenverbindungen. Die physikalisch-biogeochemischen Arbeiten, welche eng mit der nachfolgenden Fahrt M137 verknüpft waren, fokussierten auf einem Schnitt parallel zur Küste bei 12°S. Zusätzlich wurde ein Schnitt bei 14°S und ein Auftriebsfilament bei 15°S, 77°W beprobt. Das benthisch-pelagische Messprogramm umfasste CTD Profilmessungen mit Wasserprobenentnahme, schiffgebundene Turbulenz- und Geschwindigkeitsprofilmessungen, autonome hydrographische und Sauerstoffmessungen durch fünf Ozeangleiter, die Aufnahme von Strömungs- und Schichtungszeitserien durch Verankerungen, benthische in situ Nährstoff- und Spurenmetallflussmessungen und Sedimentprobenentnahme durch Lander und Multicorer, Probenentnahme durch treibende Sedimentfallen und Entnahme von Proben für Spurenstoffisotopenmessungen durch in situ Pumpen. Das Messprogramm wurde erfolgreich und wie geplant abgeschlossen.

2 Participants

2.1 Principal investigators

Name	Institution
Dengler, Marcus, Dr.	GEOMAR
Sommer, Stefan, Dr.	GEOMAR
Achterberg, Eric, Prof., Dr.	GEOMAR
Dale, Andrew, Dr.	GEOMAR
Engel, Anja, Prof., Dr.	GEOMAR
Krahmann, Gerd, Dr.	GEOMAR
Lavik, Gaute, Dr.	MPI Bremen
Thomsen, Sören, Dr.	GEOMAR

2.2 Scientific party

Name	Discipline	Institution
Dengler, Marcus, Dr	Chief scientist, MSS, moorings, lander	GEOMAR
Achterberg, Eric, Prof., Dr.	Trace metals, Fe dynamics, DOP, DON	GEOMAR
Beck, Antje	BIGO Lander, O_2, nutrients, technician	GEOMAR
Bristow, Laura, Dr.	Particles, N_2-fix, N-loss, incubations	MPI-Bremen
Cisternas-Novoa, Carolina, Dr.	Particle traps, biological oceanography	GEOMAR
Clemens, David	BIGO Lander, N-geochemistry	GEOMAR
Dale, Andy, Dr.	BIGO Lander, MUC, N-geochemistry	GEOMAR
Hopwood, Mark, Dr.	Trace metals, Fe dynamics, Phosp., DOP, DON	GEOMAR
Karthäuser, Clarissa	Particles, incubations, N_2-fix, N-loss	MPI-Bremen
Klüver, Tanja	DOM, cell activity, technician	GEOMAR
Krahmann, Gerd, Dr.	Glider, CTD, salinometers, physical oceanogr.	GEOMAR
Lavik, Gaute, Dr.	Particles, N_2-fix, N-loss, incubations	MPI-Bremen
Le Moigne, Frederic, Dr.	Particle traps, biological oceanography	GEOMAR
Lüdke, Jan	ADCP. physical oceanography	GEOMAR
Massmig, Marie	DOM, cell activity	GEOMAR
Papenburg, Uwe	Mooring, CTD, MSS, technician	GEOMAR
Petersen, Asmus	BIGO lander, MUC, mechanics, technician	GEOMAR
Plass, Anna	Benthic Fe geochemistry, MUC, BIGO lander	GEOMAR
Raeke, Andreas	Bordwetterwarte, technician	DWD
Rentsch, Harald	Bordwetterwarte	DWD
Roa, Jon	Particle traps, technician	GEOMAR
Scholz, Florian, Dr.	Benthic Fe geochemistry, MUC, BIGO lander	GEOMAR
Schüßler, Gabriele	Geochemistry, nutrients, technician	GEOMAR
Sommer, Stefan, Dr.	BIGO lander, biogeochemistry	GEOMAR
Surberg, Regina	Geochemistry, nutrients, technician	GEOMAR
Thomsen, Sören, Dr.	u-CTD, glider, physical oceanography	GEOMAR
Türk, Matthias	BIGO Lander, MUC, electronics, technician	GEOMAR
Vosteen, Paul	Geochemistry	GEOMAR
Xie, Ruifang, Dr.	Thorium, in situ pumps	GEOMAR

2.3 Participating institutions

Name	Institution
GEOMAR	Helmholtz-Zentrum für Ozeanforschung Kiel
DWD	Deutscher Wetterdienst, Geschäftsfeld Seeschifffahrt
MPI Bremen	Max-Planck-Institut für Marine Mikrobiologie

2.4 Crew

Name	Rank
Schubert, Jan F.	Kapitän / Master
Reinstädler, Marko	Ltd. Naut. Offizier / Chief Officer
Göbel, Jens	Erster Naut. Offizier / 1st Officer
Werner, Lena	Zweiter Naut. Offizier / 2nd Officer
Rathnow, Klaus	Schiffsarzt / Ship's doctor
Neumann, Peter	Leiter der Maschine / Chief Engineer
Brandt, Björn	2. Techn. Off. / 2nd Engineer
Heitzer, Ralf	2. Techn. Off. / 2nd Engineer
Starke, Wolfgang	Elektriker / Electrician
Willms, Olaf	Ltd. Elektroniker / Chief Electronics Engineer
Hebold, Catharina	Elektroniker / Electronics Engineer
Bagyura, Bernhard	System Manager / System Manager
Lange, Gerhard	Deckschlosser / Fitter
Krüger, Frank	Motorenwärter / Motorman
Schroeder, Manfred	Motorenwärter / Motorman
Kudraß, Klaus	Motorenwärter / Motorman
Wolf, Alexander	Bootsmann / Bosun
de Moliner, Ralf	Schiffsmechaniker / SM
Zeigert, Michael	Schiffsmechaniker / SM
Durst, Planung	Schiffsmechaniker / SM
Bußmann, Piotr	Schiffsmechaniker / SM
Behlke, Hans-Joachim	Schiffsmechaniker / SM
Hampel, Ulrich	Schiffsmechaniker / SM
Drakopoulos, Evgenios	Schiffsmechaniker / SM
Wernitz, Peter	Koch / Chief Cook
Fröhlich, Mike	2. Koch / 2nd Cook
Wege, Andreas	1. Steward / Chief Steward
Jürgens, Monika	Steward / Steward
Parlow, Jan	Steward / Steward
Zhang, Guomin	Wäscher / Laundryman
Schweiger, Sophia	Auszubildender / Apprentice
Staffeldt, Felix	Auszubildender / Apprentice

3 Research program

3.1 Aims of the cruise

The research cruise to the Peruvian oxygen minimum zone was carried out within the framework of the DFG Collaborative Research Centre (SFB) 754 „Climate-Biogeochemical Interactions in the Tropical Ocean“. The overarching goal of the cruise was to investigate benthic and pelagic cycling of nutrients, oxygen, and trace metals. Specific objectives were to:

- quantify the effect of benthic nutrient release on the nutrient inventories in the water column and its feedback on primary productivity at the near surface;
- quantify pelagic cycling of nutrients, oxygen, and trace metals;
- investigate how particle load and oxygen transport within particles from the euphotic zone regulate the nutrient cycling;
- determine effects of anoxia on particle remineralisation rates, elemental stoichiometry, and on patterns of organic geochemical tracer changes during the degradation process;
- quantify the role of oxygen and dissolved organic matter transport by submesoscale subduction processes;
- improve understanding of organic matter availability to heterotrophic bacteria in oxygen minimum zones;
- determine iron fluxes and mechanisms of iron stabilization, removal and recycling, with an emphasis on the effects of spatial and temporal variations in redox conditions in the water column.

3.2 Agenda of the cruise and description of the work area

To improve quantitative understanding of nutrient loss and nutrient cycling in the ocean, physical and biogeochemical observational approaches were combined. In the physical approach, observations were carried out to construct nutrient, oxygen, and trace metal flux budgets. This involves determining turbulent, lateral-diffusive and advective solute (i.e. nutrient, oxygen, and trace metal) fluxes in the water column and combining these with in-situ flux measurements across the sediment interface. To achieve this objective, moorings measuring velocity and hydrography as well as gliders were deployed and shipboard sampling of velocity, turbulence and hydrography was carried out along with solute concentration measurements. Furthermore, biogeochemical measurement techniques were used to directly determine rates of microbial nitrogen transformations by incubations. A particular focus of this pelagic biogeochemical programme was to investigate how particle load and oxygen transport within particles from the euphotic zone regulate the nutrient cycling. On several stations, sinking particles about to enter the anoxic water column were collected using a large water bottle (Snow Catcher). In situ benthic nutrient fluxes were determined with Biogeochemical Observatory (BIGO) landers equipped with benthic chambers. Along the continental slope and shelf of the 12°S transect, 9 BIGO lander stations were carried out at different water depth between 75 m and 1000 m. The benthic flux measurements were complemented by geochemical porewater analysis of sediment cores collected during Multicorer deployments.

Nutrient loss is fuelled by the export flux of organic matter. However, quantitative estimates of export fluxes in OMZs are still sparse. To investigate effects of anoxia on particle

remineralisation rates two different approaches were used: particulate organic matter was collected in different depths of the water column using drifting sediment traps and large volume pumps were deployed from the vessel for thorium isotope measurements in the water column.

A 3-day process study was carried out in upwelling filaments to investigate the interplay of biogeochemical processes in frontal zones that included high-resolution hydrography sampling as well as taking water samples for biogeochemical analysis. This data set should allow to investigate the role of oxygen and dissolved organic matter transport by submesoscale subduction processes. Finally, an iron-free CTD system (TM-CTD) having its own winch and a trace metal free wire was used to collect water samples for trace metal analysis. This data, along with the other data sets collected during the cruise shed new light on iron dynamics in OMZs.

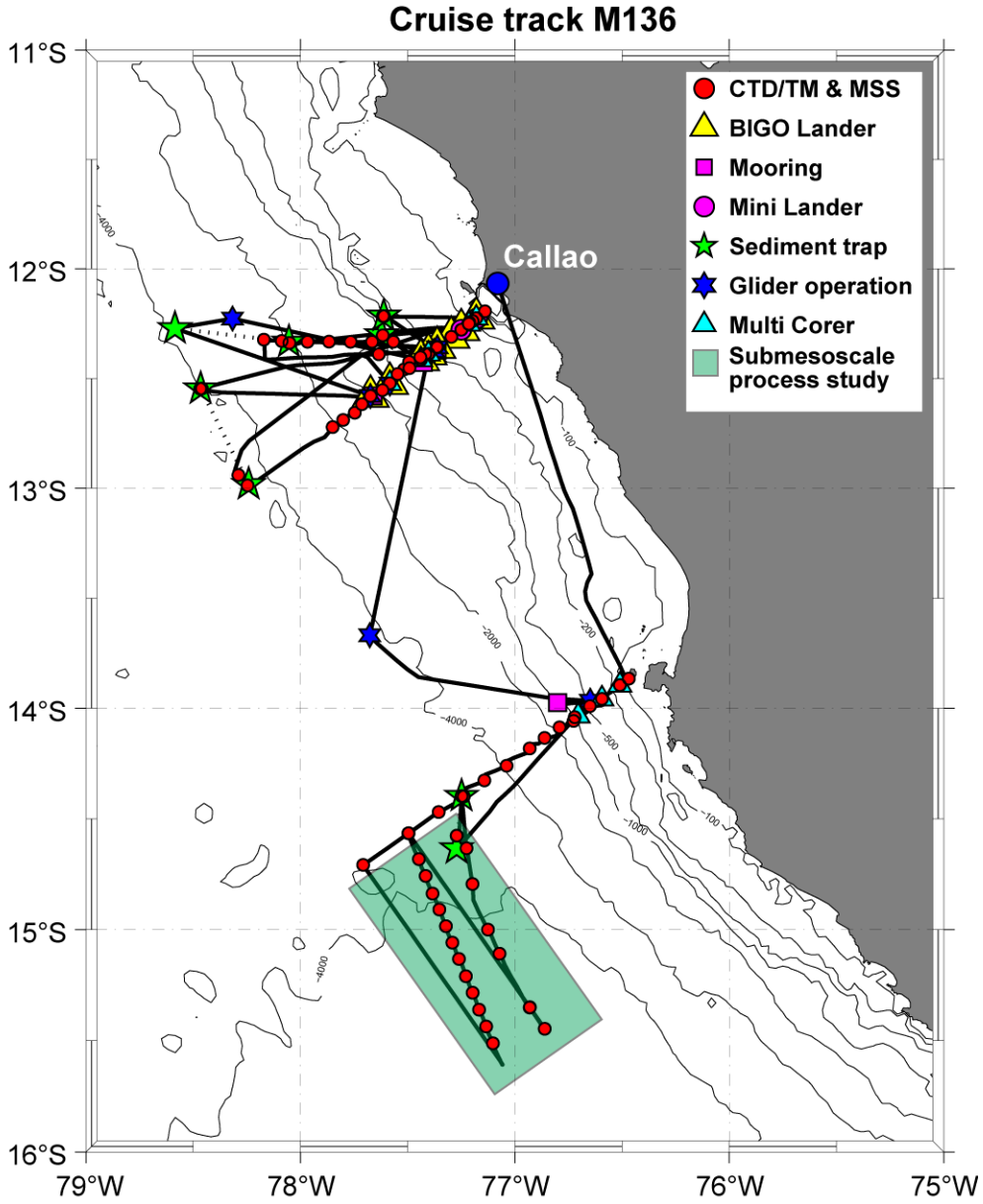

Fig. 3.1 Bathymetric map with cruise track of R/V METEOR cruise M136 (black solid line) including locations of CTD stations, Biogeochemical Observatory (BIGO) Lander, mooring and Mini Lander deployments, sediment trap deployments and recoveries, glider operations and Multicorer stations. The region of the submesoscale process study is contoured in light green.

In accordance with the ship time proposal, we successfully conducted measurements at all planned stations. We followed the DFG regulations summarized in the „Erklärung zu einer verantwortungsvollen Meeresforschung“ and the (OSPAR) Code „Code of Conduct for Responsible Marine Research in the Deep Seas and High Seas of the OSPAR Maritime Area” to avoid unnecessary environmental and ecosystem disturbances. The impact of the conducted work to the environment was very minor. All deployed instruments including moorings, gliders and landers, were recovered on this or the follow-up cruises. There were no activities, which could lead to substantial physical, chemical, biological or geological changes or damage of marine habitats. Care was taken to avoid activities, which could disturb the experiments and observations of other scientists. We made use of the most environmentally-friendly and appropriate study methods, which are presently available, and avoided collecting data that are not essential to conduct the scientific research. The number of samples was reduced to the necessary minimum.

4 Narrative of the cruise

One day before the departure from Callao port, a reception was held on R/V METEOR. It was nicely arranged by the German Embassy in Lima, Peru. About 80 guests joined the reception from different departments of the Peruvian government, colleagues from Peruvian research institutions, and employees of the German Embassy including vice Ambassador Schmidt. We were particularly happy about the visit of vice Minister for Production Hector Soldi and the President of the Peruvian marine research institution IMARPE Admiral Javier Gaviola. The reception was a great success and was complemented upon by our guests.

R/V METEOR left Callao port at noon local time on April 11 and headed south to complete a transect perpendicular to the coastline at 14°S (Fig. 3.1). Weather and sea conditions were excellent during the first 10 days when significant seas of 1 m to 2 m and southeasterly trade winds between 3 Bft. and 5 Bft. were experienced. Measurements along the 14°S transect started in the early morning of April 12 and included conductivity-temperature-depth-oxygen (CTD/O_2) profiles and water sampling using Niskin bottles that was analyzed for nutrients and various other biogeochemical parameters. A metal-free CTD/O_2 system having its own winch was used to collect water samples for trace metals concentration analysis in the water column. Usually, one trace metal CTD/O_2 (TM-CTD/O_2) profile was collected each day. Additionally, ship-board microstructure measurements, upper-ocean velocity measurements using R/V METEORs’ Ocean Surveyors, sediment sampling with a Multicorer, particle sampling with a Snow Catcher and thorium sampling using large volume in situ pumps were performed. In the evening of April 12, a mooring with an acoustic Doppler current profiler attached was successfully deployed at 1000 m depth about 5 nm to the north of the transect. Subsequently, the 14°S transect was continued. R/V METEOR arrived at the 5000 m isobath in the morning of April 14, where a drifting sediment trap was deployed.

For the next 3 days, a submesoscale process study (SMPS) was performed to the south of the transect investigating the physical-biogeochemical interaction at fronts and filaments. Satellite sea surface temperature data and real-time data from gliders deployed during the previous cruise in the 14°S region indicated that temperature and salinity fronts were located further offshore than we had anticipated during cruise planning. The sampling region for the SMPS was thus relocated to the region between 14.5°S, 77.8°W and 15.5°S, 76.6°W. Sampling included

underway CTD profiles using the Rapid Cast system, shipboard velocity measurements and CTD/O_2 profiles including water sampling that was analyzed nutrients, dissolved organic matter, primary productivity, rates of microbial nitrogen transformations via incubations and trace metals. In total, two CTD/O_2 transects and 4 underway CTD transects were competed. In the morning of April 17, the drifting sediment trap deployed three days earlier was recovered about 10 nm to the south of the deployment position. The SMPS was terminated at 15:30 UTC on April 17. After taking a last Multicorer at 800 m depth on the continental slope, the 14°S transect was completed.

While heading towards the main transect at 12°S, two gliders were recovered. The position of the first glider (IFM12) was reached in the late afternoon following the Multicorer station. The second glider (IFM09) had reported difficulties during ascent in the morning of April 17. Since then, it had remained at the sea surface. R/V METEOR arrived at the glider's position at 23:00 local time and despite darkness, the recovery went very well. It turned out that water had leaked into the nose cone of the microstructure probe attached to the glider. The fast recovery of the package prevented further damage or loss of the instruments.

The main working area at 12°S was reached at 13:00 UTC on April 18. The working schedule along the 12°S transect was predominately constrained by eight 40-hour long deployments of the BIGO landers, four 3 to 6-day deployments of drifting sediment traps, four mooring deployments, glider operations, and sediment sampling using the multi corer that all needed to be conducted during day time. During night time, the measurement program focused on CTD/O_2 and TM-CTD/O_2 profiling including water sampling, additional water sampling using a bottom water sampling device, particle sampling using a Snow Catcher, intensive microstructure profiling and trace element sampling using large volume in situ pumps.

The coordinated benthic and pelagic sampling concentrated on different water depths along the transect. The location of the stations was chosen based on oxygen and nutrient distributions and on expected benthic providences. On the shelf, benthic - pelagic sampling stations were selected at 75 m, 128 m, 143 m, and 200 m water depth, while along the continental slope stations at 240 m, 300 m, 750 m and 1000 m were sampled. Sampling at these sites included BIGO lander deployments, CTD/O_2 profiling and water sampling that were analyzed for oxygen, nutrients, nutrient cycling rates, primary productivity and trace metal concentrations. Additionally, in situ pump deployments were carried out to determine export rates, a bottom water sampler was used at some of these stations to determine near-bottom nutrient gradients and particles were collected with the Snow Catcher. Microstructure profiling combined with CTD/O_2 and nutrient sampling was frequently repeated at these sites to allow for determining diffusive nutrient fluxes due to turbulent mixing. Finally, sediment cores using the Multicorer were taken to complement nutrient and trace metal sampling at these sites.

Moorings with attached acoustic Doppler current profiler and a McLane Moored Profiler were deployed and distributed along the continental slope to allow for determining the role of nutrient advection by the boundary currents. Furthermore, the pelagic measurement program was supported by autonomous glider measurements with additional turbulence and nitrate sensors that sampled a 12°S transect 5 nm to the north of the main transect to avoid collision with the research vessel. Altogether, 6 glider operations were performed in the region of 12°S. The coordinated benthic –pelagic sampling program started with the deployment of a BIGO lander at the 240 m in the late afternoon on April 18 and was terminated after taking sediment samples

with a Multicorer in the morning of May 2. All deployments/recoveries and station measurements within the coordinated sampling were carried out successfully.

Drifting sediment trap deployments along the 12°S transect started in the afternoon of April 20 with a deployment in a water depth of 500 m. Two days later, a second trap was deployed at the outermost position of the transect at 5000 m water depth before the 500 m trap was successfully recovered in the morning of April 24. The analyzed upper ocean velocity data from R/V METEOR's ocean surveyors and also the surface drift of the 500 m trap had indicated an unexpected but persistent onshore flow during the first week of sampling along the 12°S transect. The onshore flow originated from the presence of an anticyclonic subsurface mesoscale eddy having its center about 30 nm to the north of the 12°S transect. The eddy had just recently been formed, presumably by an instability process of the Peruvian Undercurrent. To investigate the characteristics of the eddy, a physical-biogeochemical station in the center of the eddy center was carried out in the afternoon of April 26. This station included the deployment of the fourth sediment trap at about 2000 m water depth and in situ pump measurements. Eddy sampling was concluded after a zonal CTD/O_2 transect across the inshore flank of the eddy along a 12°20'S that included nutrient concentration measurements during the night of April 26. The 5000 m trap was recovered after 7 days 30 nm to the north of deployment position in the evening of April 29. The sediment trap released in the eddy center drifted to west and was recovered 40 nm away from its release position on April 30.

The work program was completed at 21:30 UTC on May 2. The cruise was terminated as scheduled in Callao port at 14:00 UTC on May 3.

5 Preliminary results

5.1 Hydrographic observations

5.1.1 CTD/O_2 system and calibration

(M. Dengler, G. Krahman, S. Thomsen, J. Lüdke)

A total number of 99 CTD profiles were collected in most cases to full ocean depth. Positions and profiling depth of the casts are detailed in section 7.1. During the whole cruise the GEOMAR SBE7, a Seabird Electronics (SBE) 9plus underwater unit, was used. It was attached to a GO4 rosette frame. The SBE7 was equipped with one Digiquartz pressure sensor (s/n 1162) and double sensor packages for temperature (T), conductivity (C) and oxygen (O) (primary set: T1 = s/n 4051, C1 = s/n 2512, O1 = s/n 2669; secondary set: T2 = s/n 2120, C2 = s/n 3374, O2 = s/n 992). Additionally, fluorescence and turbidity sensors (Wetlabs), a sensor measuring photosynthetically active radiation (PAR) and a sensor measuring nitrate concentrations were attached to the SBE7. To collect water samples, 24 10-liter bottles were attached to the rosette frame. All sensors worked well throughout the cruise. Data acquisition was done using Seabird Seasave software version 7.23.2.

For calibration of the CTD conductivity and oxygen sensors, conductivity values were determined from 109 water samples using a Guildline Autosal salinometer (AS) and oxygen concentrations were determined from 248 water samples using Winkler titration. Throughout this cruise, conductivity values from the water samples were analyzed using the GEOMAR salinometer AS 8 (Model 8400 B). Only small adjustments to the standardization potentiometer of the salinometers were necessary during the cruises and subsequent sub-standards

determinations within each measurement day indicated an adequate stability of the instrument. For Winkler titration measurements, the same measurement setup and titration procedures as during M135 and M137 were used. For details, the reader is referred to section 5.2.1 in the M135 cruise report (Visbeck et al., submitted).

CTD conductivity was calibrated using linear dependencies of pressure, temperature and conductivity to match the salinometer-derived values. To increase accuracy of the calibration, salinometer-derived values from M135 and M137 were additionally used for the calibration of the conductivity sensors, as the same sensors were used during all three cruises. CTD oxygen was calibrated using linear dependencies of pressure, temperature and oxygen as well as 2nd order in oxygen and the product of oxygen and pressure. The misfit, taken here as the root-mean square (rms) of the differences between CTD values and the respective water samples, was 0.00010 S/m and 0.00010 S/m for the C_1 and C_2 sensors, respectively. The conductivity misfit translates into a salinity misfit of 0.0010 psu and 0.0010 psu. The misfits for O_1 and O_2 sensors on M136 were 0.39 and 0.38 µmol kg^{-1}, respectively. For each fit, the 33% most deviating water samples values were removed to exclude biases by bad samples. For the final data set that will also be publicly available, the primary sensor set was used for all CTD stations. Data from the fluorescence and turbidity sensors and the PAR sensor were calibrated by the calibration coefficients provided by the manufacturer. No further corrections were applied. Data from nitrate sensor (type SUNA, manufactured by Seabird Satlantic, s/n 761) were calibrated against 1149 nitrate measurements made from water samples. The independently collected and processed nitrate data from the SUNA sensor was later merged with the CTD data.

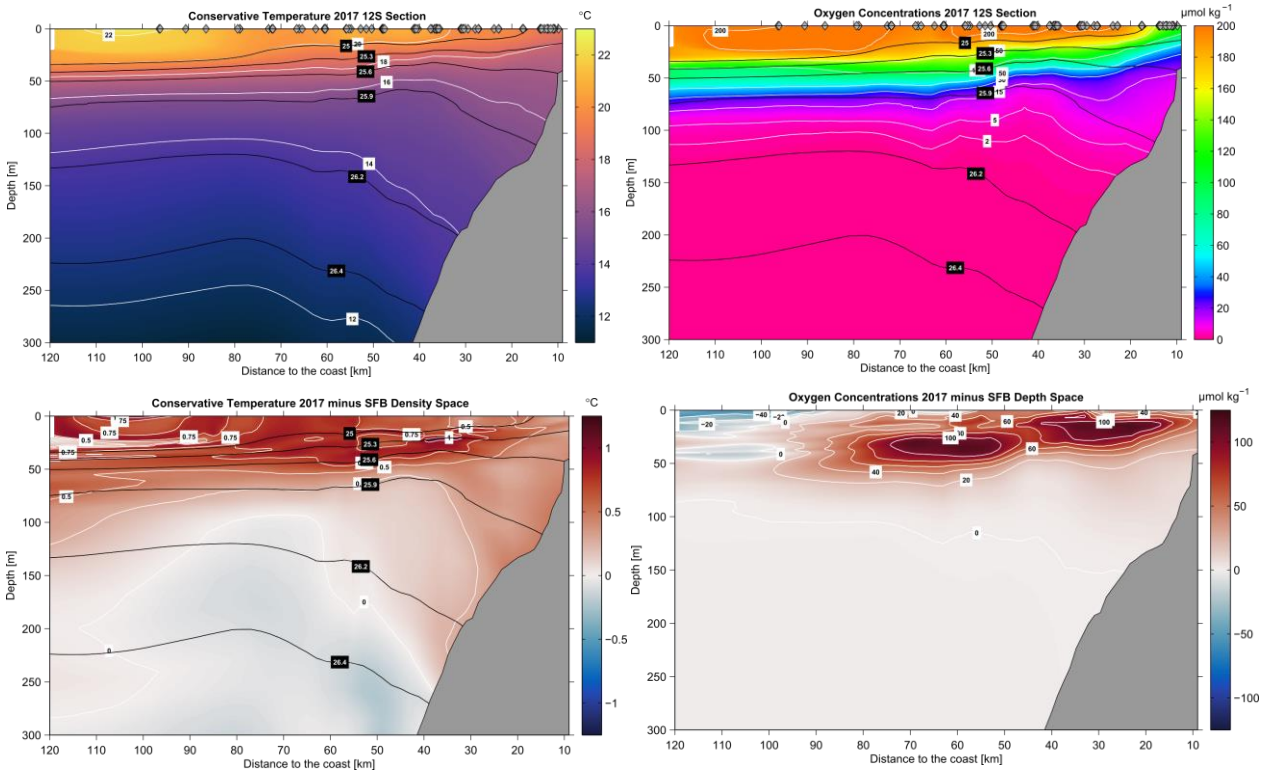

Fig. 5.1: Distance to coast - depth distribution of conservative temperature (upper left panel) and oxygen concentration (upper right panel) along the transect 12°S. Diamonds above the plot mark positions of CTD stations. Black contours indicate isopycnals (σ_θ) in kg m^{-3}. Lower panels show temperature difference (left panel) and oxygen concentration differences (right panel) across the 12°S section between the data collect during January-March 2013 (R/V METEOR M92 and M93 cruises) and the data collected during M136.

CTD/O_2 system preliminary results:

In the upper ocean along the 12°S transect, we encountered anomalously warm, saline, and oxygenated waters in comparison to previous cruises. Waters in the upper 80m were about 1°C warmer (Fig. 5.1) and between 0.02 psu and 0.03 psu richer in salinity compared to hydrographic data from 12°S collected during austral summer 2013. This anomalous water mass was also rich in oxygen leading to oxygenated waters above the upper continental slope and shelf in depth shallower than 100m (Fig. 5.1). In contrast, during the previous cruises mentioned above, waters above the upper continental slope and shelf below 30m depth were found to be anoxic (e.g. Thomsen et al., 2016).

We presume that the anomalous water mass is linked to the coastal El Niño event that had occurred in northern Peru just a few weeks prior to the cruise. The coastal El Niño event was associated with heavy rainfall that led to land-sliding and extensive flooding in northern Peru. A first analysis suggests that the anomalous water mass likely originated from above the EUC core at the equator and was rapidly advected southward along the continental margin off Peru, perhaps by coastally trapped waves (e.g. Pietri et al., 2014).

5.1.2 Underway-CTD/Rapidcast measurements and calibration

(S. Thomsen, M. Dengler, G. Krahmann)

The underway RapidCast system allows continuous and autonomous sampling of temperature, salinity and pressure while the vessel is steaming. For measurements from the surface to depth of 100 m, a profile can be obtained about every 4 minutes while the vessel is moving at 10 knots. During the cruise, the RapidCast was deployed during transit and to survey the upper ocean for submesoscale filaments and fronts (Fig. 5.2). A total of 1225 underway

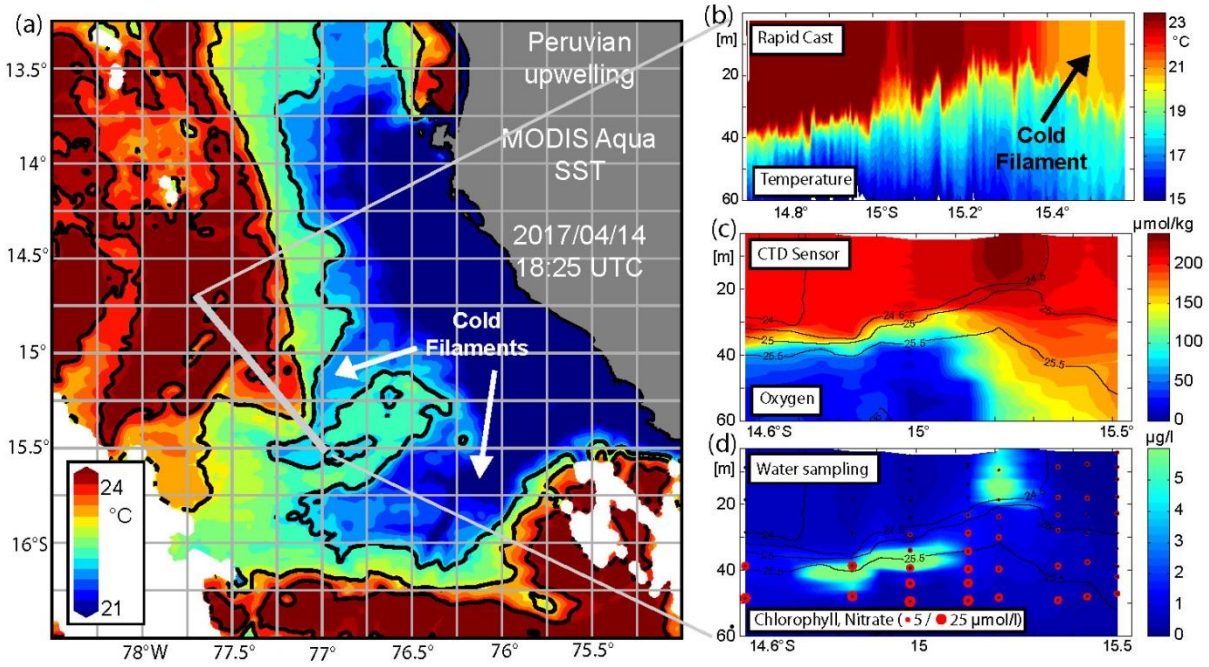

Fig. 5.2: (a) Satellite sea surface temperature from April 14, 2019 showing two cold filaments in the region of the submesoscale process study off Peru. (b) High-resolution temperature transect measured with the underway RapidCast system, (c) oxygen concentrations along the same transect as in but measured with the CTD/Rosette system, and (d) Chlorophyll *a* (CTD Sensor) and nitrate concentrations (water samples) across a cold filament.

conductivity-temperature-depth (uCTD) profiles were collected during 19 deployments (see section 7.1). Two different uCTD probes (s/n 54 and 155) measuring and internally recording pressure, temperature and conductivity were used along with Teledyne RapidCast system. For the calibration of the sensors, the probes were attached to the CTD rosette during calibration casts. Fortunately, pressure offsets were found to be very small. The subsequent calibration of temperature and salinity included a thermal lag correction and a temporal drift analysis from the comparison between the CTD-calibrated thermosalinograph data and the uCTD surface measurements. It was found that only the salinity of s/n 155 required the addition of a small offset of -0.005 PSU to match the thermosalinograph values. In neither probe a temporal drift of the sensor readings was diagnosed.

One aim of our observational program was to advance understanding on the coupling between physical and biogeochemical processes. Enhanced coupling is expected to occur in the mixed layer at sharp temperature fronts and within cold filaments. We captured these structures with the RapidCast system by measuring hydrography at high-spatial and temporal resolution (Fig. 5.2). In our optimized sampling strategy, we first identified the exact positions of the features of interest using the RapidCast data and the subsequently sampled biogeochemical parameters within the features.

5.1.3 Thermosalinograph

(G. Krahmann, M. Dengler)

Sea surface temperature (SST) and sea surface salinity (SSS) were continuously measured by the ship's dual thermosalinograph. The system consists of two devices, one with an inlet at the starboard side (TSG1) and the second with an inlet at the portside (TSG2). The area off Peru is difficult for these systems as clogging occasionally limits the water flow in the systems. Additionally, the strong biological activity leads to elevated drifts of the sensor readings when bio-fouling occurs within the system. The calibration of TSG1 and TSG2 salinities was separated into 2 time intervals. TSG1 required 2nd order time dependent drift corrections, while for TSG2 two constant offsets were sufficient for the two time intervals.

All four temperature sensors (T_1 through T_4) and both conductivity sensors (S_1, S_2) were calibrated against the 5 dbar values from the 99 CTD profiles taken during the cruise. Estimated uncertainties are ±0.0179°C (T_1), ±0.0157°C (T_2), ±0.0179°C (T_3), ±0.0136°C (T_4), ±0.006 (S_1), and ±0.007 (S_2).

5.1.4 Glider operations

(G. Krahmann, M. Dengler, S. Thomsen)

An integral component of the measurement program was the use of autonomous platforms (ocean gliders) measuring hydrography, turbulence, and various biogeochemical parameters at high spatial resolution across the continental slope. Altogether, five Slocum gliders (ifm03, ifm07, ifm09, ifm12, ifm13) were used during eight glider deployments (Fig. 5.3, Tab. 5.1). The measurement program started with the deployment of two gliders (ifm12 and ifm09) during R/V METEOR cruise M135 on April 3, 2017 and was completed after the recovery of ifm09 (3rd mission) during R/V METEOR cruise M138 on June 11, 2017.

All gliders were equipped with temperature, conductivity, pressure, chlorophyll (chl-*a*), turbidity and oxygen sensors. Apart from the sensors built into the gliders, four of the five gliders carried self-contained sensor packages mounted to the gliders' top (Tab. 5.1). Ifm03 and

ifm09 were equipped with a microstructure probe (MicroRider, Rockland Scientific) with two microstructure shear and two microstructure temperature sensors as well as fast-responding accelerometers while ifm12 and ifm13 was equipped with an optical nitrate sensor (SUNA, Satlantic). All internal and external sensors of the gliders worked well throughout the missions.

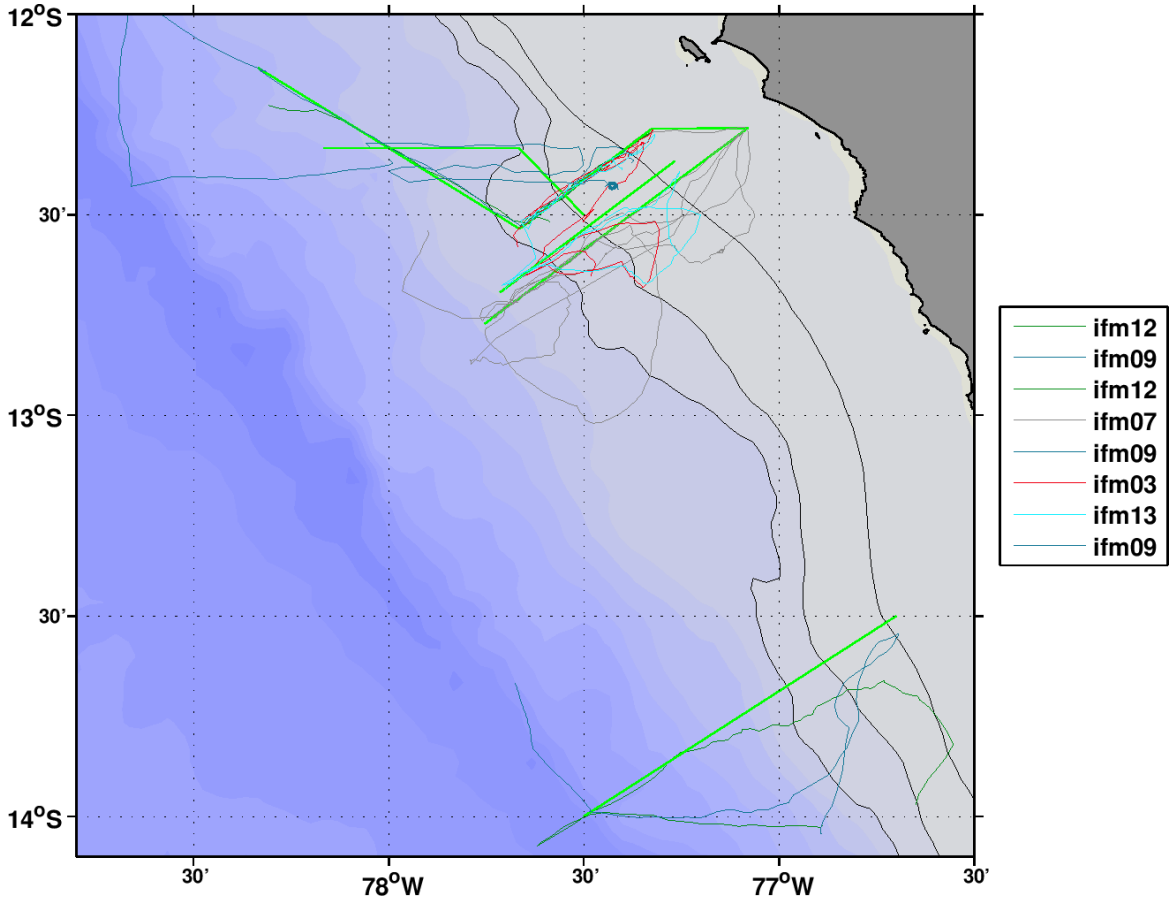

Fig. 5.3: Tracks of the eight glider missions carried out during the glider measurement program.

During the cruise, 8 glider operations were carried out. Glider ifm09 and ifm12 were recovered at the beginning of the cruise shortly after completing the 14°S transect on April 17 and 18, respectively. The batteries of both glider were replaced, gliders were cleaned and goose barnacles and seaweed were removed that had slowed down the gliders earlier. On April 20, ifm03 was deployed in 750m water depth at the 12°S section. Three days later on April 23, the shallow water glider ifm07 was deployed on the upper continental slope at 12°S. ifm09 was redeployed on April 25 and ifm03 was deployed on April 29. Both gliders were recovered on the

Tab. 5.1: Summary of glider missions. Abbreviations are used as follows: p- pressure, T – temperature, S – salinity, O_2 – oxygen concentration, chl-*a* – chlorophyll.

	Ifm03	**Ifm07**	**Ifm09**	**Ifm12**	**IFM13**
Mission	Depl14	Depl10	Depl09, 10, 11	Depl06, 07	Depl05
Survey area	12°S	12°S	14°S and 12°S	14°S and 12°S	12°S
Deployment date	Apr. 29, 21:30	Apr. 23, 19:00	Apr. 3, 16:20	Apr. 3, 14:40	May 1, 22:15
Recovery date	May 23, 18:00	Jun. 10, 14:45	Jun. 11, 12:15	Apr. 29, 19:15	May 28, 14:30
Sensors	p, T, S, O_2, chl-*a*, turbidity	p, T, S, O_2, chl-*a*, turbidity	p, T, S, O_2, chl-*a*, turbidity	p, T, S, O_2, chl-*a*, turbidity	p, T, S, O_2, chl-*a*, turbidity
Mounted probes	Microstructure		Microstructure	Nitrate (SUNA)	Nitrate (SUNA)
Number of profiles	1142	5498	1894	1072	1258
Max. depth (db)	800	200	800	800	800

follow up cruise M137. Shortly before the end of the cruise on April 30 glider ifm12 was recovered. Finally, on the second to last day, glider ifm13 was deployed to be recovered on the subsequent cruise. All glider operations were carried out successfully using the rubber boat of R/V METEOR. Details of the glider swarm experiment and plots of the satellite-transmitted data can be retrieved from the GEOMAR web site https://gliderweb.geomar.de/html/swarm09.html.

5.1.5 Turbulence measurements using microstructure sensors

(M. Dengler, S. Thomsen, J. Lüdke)

A microstructure measurement program was carried out to quantify pelagic diffusive fluxes of oxygen, nutrients and other solutes due to turbulent mixing along the Peruvian continental slope and shelf. Additionally, the program aimed at advancing the understanding of the mixing processes at the continental slope and shelf. Here, tide-topography interaction generates baroclinic tides and nonlinear internal waves (e.g. Mosch et al., 2012; Erdem et al., 2016) that lead to enhanced near-bottom and near-surface mixing.

The turbulence measurement program consisted of autonomous turbulence sampling by two gliders equipped with microstructure sensors (see section 5.1.4) and of shipboard microstructure profiling system (MSS) manufactured by Sea & Sun Technology. For the ship-based microstructure measurements, two MSS90-D profiler (S/N 26 and S/N 73), a winch and a data interface was used. The loosely tethered profiler were optimized to sink at a rate of 0.55 ms^{-1}. In total, 189 profiles were collected during 45 microstructure stations. Both profilers were equipped with three shear sensors, a fast-response temperature sensor, an acceleration sensor, two tilt sensors and conductivity, temperature, depth sensors sampling with a lower response time. Additionally, profiler S/N 73 carried an optical oxygen sensor. A comparison of the CTD oxygen sensor data and the MSS oxygen sensor data showed that both sensors were able to resolve comparable small-scale variability of oxygen. The MSS oxygen sensor thus proved to be adequate to resolve the elevated oxygen gradients found in the upper water column off Peru. Shear sensors attached to profiler S/N 26 during all collected profiles were S/N130 (sh1), S/N 44 (sh2) and S/N 120 (sh3). Profiler S/N 73 was carrying S/N 134 (sh1), S/N 135 (sh2) and S/N 125 (sh3). Due to a loss of sensitivity of S/N 125, we replaced this sensor by S/N 133 prior to MSS station 28 (after S/N 73 profile 58). At the same time, the pre-amplifier of the shear channel was replaced as well.

5.2 Current observations

5.2.1 Vessel mounted acoustic Doppler current profiler

(J. Lüdke, M. Dengler)

Upper-ocean velocities along the cruise track were recorded continuously by the two vessel mounted acoustic Doppler current profiler (vmADCP) systems of R/V METEOR. The 38 kHz RDI Ocean Surveyor (OS38) system was operated in narrowband mode with 32 m bins and a blanking distance of 16 m while 55 bins were recorded. The 75 kHz RDI Ocean Surveyor (OS75) was operated in narrowband mode recording 100 bins of 8 m length and a blanking distance of 4 m. The measurement range of the OS75 was about 700 m, but due to low backscatter abundance within the OMZ, the data quality was occasionally reduced between 300 and 400 m depth. The OS38 recorded high-quality data to about 1200 m depth during the whole cruise. Both systems worked reliably throughout the cruise.

Post-processing of the data included bottom editing and a water track calibration of the misalignment angle and amplitude of the Ocean Surveyor signals (Tab. 5.2). To increase data accuracy, we combined the velocity records from M136 and the follow-up M137 for the water track calibration. As indicated by the relatively low standard deviation of the misalignment angle calibration, the collected data set was of high quality.

Tab. 5.2 Misalignment angle, amplitude factor and their uncertainties resulting water track calibration of the Ocean Surveyor data.

OS	Mode	Misalignment angle ± Standard deviation	Amplitude factor ± Standard deviation
75	NB	-1.0267 ± 0.65097	1.0054 ± 0.01314
38	NB	-0.43998 ± 0.74786	1.0037 ± 0.01519

Preliminary results vmADCP

During the cruise period, we encountered a moderate poleward Peru-Chile Undercurrent (PCUC, Fig. 5.4) that was situated above the upper continental slope and shelf at depth above 200 m within 50 km of the coast. Poleward velocities averaged between April 18 and May 2 were above 20 cm s^{-1} on the upper shelf. Maximum climatological average poleward flow within the PCUC is about 10 cm s^{-1} (Chaigneau et al., 2013).

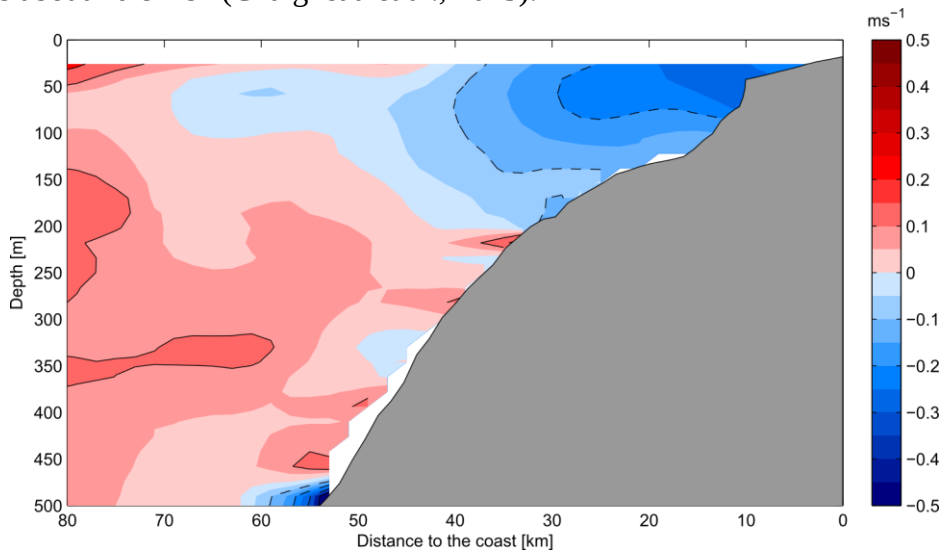

Figure 5.4: Alongshore velocity across the 12°S section averaged from all data collected between April 18 and May 2, 2017. Negative velocities (blue) indicate southeastward flow. The Peru-Chile Undercurrent is well pronounced above the upper continental slope and shelf within 40 km of the coast.

Upon arrival at the 12°S section on April 18, the vmADCP data revealed the existence of an anticyclonic subsurface eddy centered about 60 km offshore from the coast that subsequently propagated westward (Fig. 5.5). During the previous cruises in austral summer 2013, the separation of the PCUC core and subsequent evolution of an eddy was observed in detail at exactly the same position (Thomsen et al 2016). This supports previous results suggesting eddy generation to be associated with boundary layer separation of the PCUC (Marshall and Tansley, 2001). The complex topography just upstream of 12°S causes changes in the streamline curvature of the current, which facilitates separation of the flow. Subsequently, several CTD stations were taken from the eddy core to analyze its physical and biogeochemical properties.

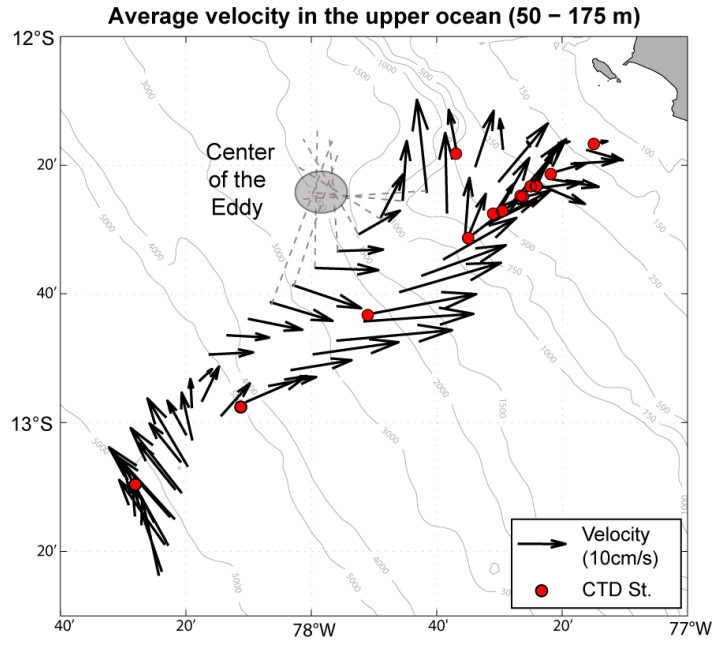

Fig. 5.5: Average currents between 50m and 175m depth (arrows). The data suggest a pronounced anticyclonic eddy north of our transect having a center at about 12°20'S, 78°W.

5.2.2 Mooorings

(M. Dengler, S. Thomsen, G. Krahmann)

A mooring program carried out during M136 and the subsequent cruises M137 and M138 to investigate the variability of the circulation and hydrography along the continental slope off Peru and to capture internal tides and non-linear internal waves propagating onto the continental slope and shelf. Altogether, four moorings and two oceanographic lander were deployed at different depth along the continental slope near the 12°S and 14°S transects (Tab. 5.3**)**. While all equipment was deployed during M136, the landers' recovery was carried out during the final days of M137 and all mooring recoveries occurred during M138. Three moorings were equipped with 300 kHz ADCPs that had target depths between 100 m and 250 m. Additionally, these mooring carried a temperature, salinity and pressure loggers and one of those moorings had a second downward-looking ADCP (1200kHz) attached. The forth mooring (KPO 1180) was equipped with a McLane moored profiler (MMP) set to climb the depth range from 15 m to 290 m every 45 minutes. The MMP records 3-D velocity and CTD data while climbing up and down the mooring cable.

Tab. 5.3 Mooring and landers deployed during M136. A backfall of 8% of the total mooring length was taken into account for determining the mooring position.

Mooring	Date and time (UTC)		Deployment position		Water depth	Parameters
	deployed	recovered	Latitude	Longitude		
KPO 1180 (moored profiler)	21.04. 14:20	24.06., 15:40 (M138)	12° 25.652'S	077°25.658'W	301 m	S, T, p, u,v
KPO 1181 (double ADCP)	19.04. 12:38	23.06., 20:33 (M138)	12° 22.288'S	077° 21.779'W	203 m	S, T, p, u,v
KPO 1182 (ADCP 250m)	28.04. 17:08	24.06., 11:14 (M138)	12° 34.732'S	077° 39.618'W	999 m	S, T, p, u,v
KPO 1183 (ADCP 100m)	14.04. 23:37	11.06., 14:18 (M138)	13° 58.414'S	076° 47.942'W	990 m	S, T, p, u,v
Lander SML	24.04. 14:47	25.05., 14:12 (M137)	12° 13.520'S	077° 10.790'W	75 m	S, T, p, u,v, O_2
Lander POZ	24.04. 16:43	25.05., 18:04 (M137)	12° 16.690'S	077° 14.992'W	127 m	S, T, p, u,v, O_2

The landers were equipped with a RDI Workhorse Sentinel 300 kHz acoustic Doppler current profiler, RBR CTD recorder, a high precision pressure sensor (accuracy of 0.015%), and an oxygen optode. All sensors worked well and delivered excellent data sets.

5.3 In situ benthic flux measurements, BIGO-I and BIGO-II

(S. Sommer, A. Beck, D. Clemens, A. Dale, A. Petersen, A. Plass, F. Scholz)

Within the Kiel SFB 754 in situ flux measurements across the benthic boundary layer were conducted during METEOR cruises M77-1/2 at a zonal transect at 11°S and along a depth transect at 12°S during M92. These previous cruises revealed that the shelf and upper slope sediments are important for enhanced nutrient release (phosphate, PO_4^{3-}, ammonium, NH_4^+, iron). However, these measurements were exclusively conducted during austral summer. Furthermore, during the M92 cruise benthic fluxes across the Peruvian margin were measured under conditions of high sulfide release from the shelf sediments and bottom waters that were depleted in nitrate (NO_3^-) and nitrite (NO_2^-).

During this and the follow-up cruise M137 our aim was to quantify benthic and pelagic fluxes during the onset of the austral winter period following the seasonal maximum of productivity. Additionally, our measurements were conducted under conditions after the strong El Niño in 2015/16 and prevailing positive sea surface temperature anomalies close to the coast. Major task was to determine natural in situ fluxes of nitrogen species (dinitrogen (N_2), NO_3^-, NO_2^-, NH_4^+) as well as PO_4^{3-}, Fe and trace metals across the sediment water interface under conditions of different bottom water oxygen (O_2), NO_3^- and NO_2^- concentrations and organic carbon content of the surface sediments.

Two structurally similar BIGO´s (BIGO I and BIGO II) were deployed as described in detail by Sommer et al. (2009). In brief, each BIGO contained two circular flux chambers (internal diameter 28.8 cm, area 651.4 cm^2). A TV-guided launching system allowed smooth placement of the observatories at selected sites on the sea floor. Four hours after the observatories were placed on the sea floor the chambers were slowly driven into the sediment (~ 30 cm h^{-1}). During this initial time period where the bottom of the chambers was not closed by the sediment, the water inside the flux chamber was periodically replaced with ambient bottom water. The water body inside the chamber was once further replaced with ambient bottom water after the chamber has been driven into the sediment to flush out solutes that might have been released from the sediment during chamber insertion. To trace nitrogen fluxes (NO_3^-, NO_2^-, NH_4^+), phosphorous and silicate release as well as total alkalinity 8 sequential water samples were removed with a glass syringe (volume of each syringe ~ 46 ml) by means of glass syringe water samplers. The syringes were connected to the chamber using 1 m long Vygon tubes with a dead volume of 5.2 ml. Prior to deployment these tubes were filled with distilled water. Another 8 water samples were taken from inside of one of the two benthic chambers using an eight-channel peristaltic pump, which slowly filled glass tubes (quartz glass). These samples were used for the gas analyses of N_2/Ar (Sommer et al. 2016) as well as DIC (Sommer et al. 2017). A further set of 8 glass tubes were used to take samples for trace metal measurements from the other chamber. To monitor the ambient bottom water geochemistry an additional syringe water sampler was employed and another series of eight glass tubes were used. The positions of the sampling ports were about 30 – 40 cm above the sediment water interface. O_2 was measured inside the chambers

and in the ambient seawater using optodes (Aandera) that were calibrated before each lander deployment.

During this cruise the glass tubes connected to chamber 1 were used for dissolved iron analyses and were filtered (filter sizes 0.2 and 5 µm) whilst sampling. In addition to the chambers and ambient bottom water vertical nutrient gradients were sampled using an arm that extended vertically from the lander into to water column allowing to sample water in vertical heights from the seafloor of 0.5, 1, 2, 3, and 4 m.

A total of 8 deployments of BIGO I and BIGO II were conducted along the 12°S transect in water depths of 76, 130, 145, 195, 243, 302, 752, and 984 m (Table 5.4). The station at around 400 m water depth was omitted since sampling in this area is difficult due to hard grounds. The samples obtained were used for pore water and solid phase analyses, flux determination of the various solutes mentioned above.

Table 5.4: Station list of BIGO I and BIGO II deployments

METEOR Station	Gear	Date and time (2017)	Latitude (S)	Longitude (W)	Depth [m]	remarks
M136-415	BIGO-II-1	18.04., 20:17	12°23.31’	77°24.17’	243	deployment patches of mats, C1 & C2 water lost
M136-430	BIGO-I-1	19.04., 20:45	12°24.89’	77°26.28’	302	rare patches of mats
M136-460	BIGO-II-2	21.04., 22:28	12°31.35’	77°34.98’	752	no mats, C2 water lost
M136-471	BIGO-I-2	23.04., 20:48	12°21.51’	77°21.71’	195	patches of mats, sediment surface distributed, C1 & C2 water lost.
M136-488	BIGO-II-3	24.04., 20:57	12°16.78’	77°15.00’	130	mats, ripples, pumps for glass tubes defect
M136-503	BIGO-I-3	25.04., 22:02	12°18.70’	77°17.79’	145	50% mat coverage
M136-533	BIGO-II-4	27.04., 21:20	12°13.49’	77°10.77’	76	seafloor not visible, pumps for glass tubes defect
M136-545	BIGO-I-4	28.04., 17:51	12°34.88’	77°40.38’	984	C1 & C2 water lost

Preliminary results benthic fluxes

Although the solute concentrations are not finally corrected, first trends of fluxes across the sediment water interface with increasing water depth and distance to the shore line can be detected (Fig. 5.6). Please note that Figure 1 contains data from the subsequent cruise M137 where stations at 74 m (M137-614 BIGO-I-1) and 244 (M137-596 BIGO-II-1) were repeated. Flux measurements at a station in 100 m water depth (M137-642 BIGO-II-2), which due to time constraints couldn’t be measured during cruise M136 are now included. These fluxes are compared to fluxes determined at the same locations during the previous cruise M92, which was conducted in austral summer (05.01 – 03.02.2013) under conditions of a sulfidic event and oxygen, nitrate and nitrite depleted bottom water on the shallow shelf.

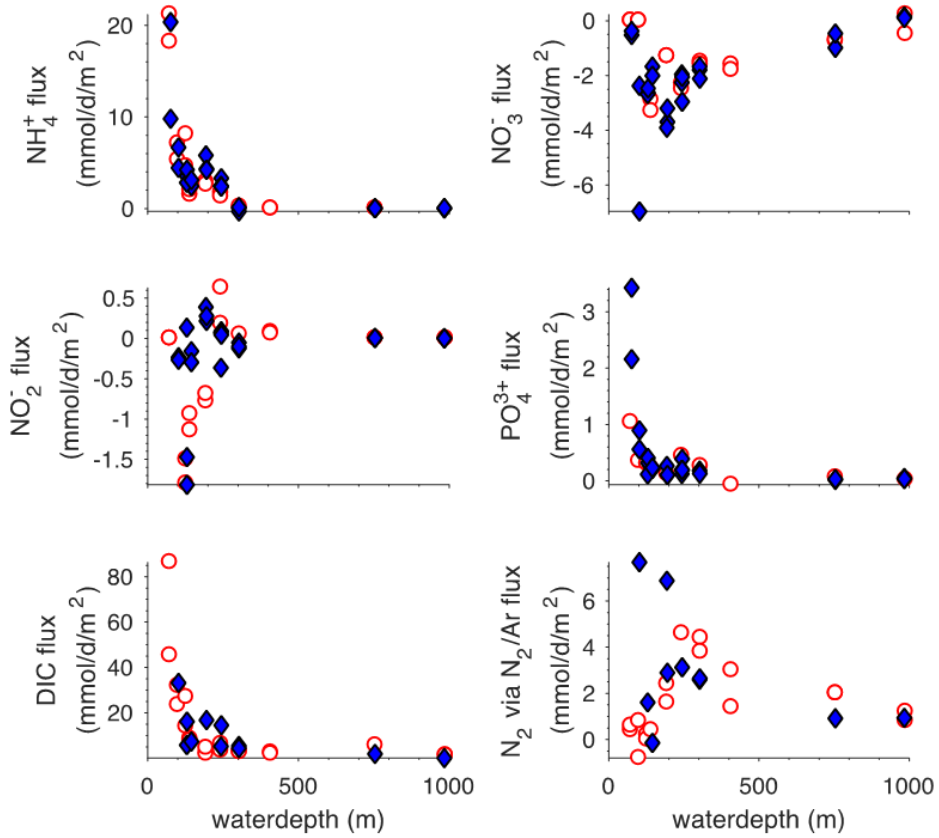

Fig. 5.6: Preliminary in situ fluxes of various solutes across the sediment water interface. Fluxes measured during cruises M136/137 are depicted as blue diamonds in comparison to those of M92 displayed as open red circles.

5.4 Porewater geochemistry

(A. W. Dale, F. Scholtz, A. Plass, B. Domeyer, G. Schüssler, M. Paul, K. Meier)

The porewater composition of surface sediments was investigated at nine stations at the 12°S transect and at three stations along the 14°S transect in order to characterize and quantify sediment diagenetic processes below the oxygen-deficient waters offshore Peru. One aim of this cruise was to further our understanding of the benthic-pelagic coupling in oxygen deficient regions of the ocean by examining key geochemical species whose chemical behaviour and distribution are altered via changes in redox potential. Specific emphasis was placed on the biogeochemical cycling of redox sensitive elements such as N, P and Fe, which are preferentially released from sediments under oxygen deficient bottom waters. The magnitude of this recycling flux, the relative importance of key control parameters, and the coupling to the carbon cycle are still poorly understood. In order to overcome this lack of knowledge, we performed geochemical analyses of pore water from surface sediments that were retrieved by multiple-corer (MUC) and benthic lander deployments (BIGO).

Sediment cores (max. ~ 40 cm in length) were retrieved using the multiple-corer (MUC) in addition to smaller push cores recovered with the BIGO landers (max. ~ 15 cm in length). An overview of the sampling stations where porewater was analyzed is given in Table 5.5. After retrieval, all cores were transferred to a cooling lab (12°C, mean bottom water temperature along the transect) and processed within 1-2 hours. Supernatant bottom water of the multiple-cores was

sampled and filtered for subsequent analyses. In general, one main MUC was taken at the same site of BIGO deployments, but not necessarily on the same day. Sediment samples from the cores sectioned in the glove bag were spun in a refrigerated centrifuge at 4000 rpm for 20 min to separate the porewater from the particulates. For all measurements and sub-sampling for redox-sensitive parameters (e.g. Fe, nutrients) from the MUC cores, the sediments were sectioned and porewaters sub-sampled in an argon filled glove bag. The sampling depth resolution increased from 1 cm at the surface to 4 cm at depth. Inside the glove bag, porewater samples were filtered with 0.2 nm cellulose-acetate filters. Porewater extraction yielded 20-50 ml of porewater at each depth interval. BIGO cores from the main (non-experimental) lander deployments were sectioned rapidly under ambient atmosphere, centrifuged, and filtered inside the glove bag. Sediment samples were also taken for the calculation of sediment density and water content as well as solid phase constituents in the onshore laboratory.

A total of 300 porewater samples were recovered and analyzed (Table 5.5) during the cruise. Porewater analyses of the following parameters were carried out on board: ferrous iron (Fe^{2+}), nitrate (NO_3^-), nitrite (NO_2^-), ammonium (NH_4^+), phosphate (PO_4^{3-}), silicate (H_4SiO_4), total alkalinity (TA) and hydrogen sulphide (H_2S). For H_2S analysis, an aliquot of pore water was diluted with appropriate amounts of oxygen-free artificial seawater and the sulphide was fixed by immediate addition of zinc acetate gelatine solution immediately after pore-water recovery. NO_3^- and NO_2^- were determined on a Quaatro Autoanalyzer (Seal Analytic) using standard methods (Grasshoff et al., 1999) with detection limits of 30 and 5 nM set by the lowest calibration standards, respectively. NH_4^+, PO_4^{3-}, H_4SiO_4 and H_2S nitrate were determined on a Hitachi U-2001 spectrophotometer with detection limits of 2, 5, 1 and 1 µM (respectively). For the analysis of dissolved Fe^{2+} concentrations, sub-samples of 1 ml were taken within the glove bag, immediately stabilized with ascorbic acid and later analysed after complexation with 20 µl of Ferrozin. The precision of this assay was <2 %. Samples for TA were analyzed by titration of 0.5-1 ml pore water according to Ivanenkov and Lyakhin (1978). Titration was ended when a stable pink colour appeared. During titration, the sample was degassed by continuously bubbling nitrogen to remove any generated CO_2 and H_2S. The acid was standardized using an IAPSO seawater solution. The detection limit and precision of the method is 0.05 meq L^{-1}.

Untreated samples were also stored in a refrigerator for onshore analysis of chloride, bromide, and sulphate by ion-chromatography. Acidified sub-samples (3-8 ml with 1% v/v concentrated trace metal grade nitric acid) were prepared for analyses of major ions (K, Li, B, Mg, Ca, Sr, Mn, Br, and I) and trace metals by inductively coupled plasma optical emission spectroscopy (ICP-OES) and inductively coupled plasma mass spectrometry (ICP-MS). Samples for DIC and stable N isotopes (^{15}N, ^{14}N) will also be determined on selected sub-samples in the shore-based laboratories.

Preliminary results porewater geochemistry

Overall, the porewater data resemble the trends observed at the same stations during cruise M92 in 2013 on board RV METEOR (Dale et al., 2016). A notable exception was found for the shallowest station on the shelf (Fig. 5.7). Whereas in 2013 the surface sediments were covered with thick mats of filamentous sulfide oxidizing bacteria *Thioploca* spp., during M136 the sediments were devoid of conspicuous surface mats. It is striking that the absence of mats is associated with vastly different concentrations of PO_4^{3-}, Fe^{2+} and H_2S in the upper 20 cm, which suggests a direct or indirect role of the bacteria in modulating the levels of these solutes in the

porewater. The absence of mats during the present cruise is probably caused by the strong El Niño event in 2015/2016 which is known to ventilate shelf waters and cause a decline in microbial biomass (Gutiérrez et al., 2008). Most likely, a decline in the rate of sulfide oxidation due to the diminished *Thioploca* community explains the build-up of H_2S in the porewater. These data will be further complemented with solid phase analyses and numerical reaction-transport model simulations to quantify the relative importance of *Thioploca* and similar organisms to benthic solute exchange at 12°S on the Peruvian margin (e.g. Bohlen et al., 2011).

Table 5.5: Stations for geochemical analysis of porewaters from multiple-corer (MUC) and benthic lander (BIGO, chamber 1 (C1) or chamber 2 (C2)) samples listed by water depth. BIGO cores are marked in blue for clarity. Note that sediments from 3 stations (338, 342 and 409) were recovered at 14°S, whereas all other deployments were made at 12°S.

Station No.		Depth	Date	Latitude	Longitude	No. of
METEOR	GEOMAR†	[m]	2017	[°S]	[°W]	samples
M136-483	MUC8	75	24.04.	12°13.52’	077°10.79’	14
M136-483	MUC 8 DOM	75	24.04.	12°13.52’	077°10.79’	17
M136-533	BIGO II-4 C1	75	27.04.	12°13.50’	077°10.78’	10
M136-577	MUC11 DOM	105	01.05.	12°15.14’	077°12.88’	14
M136-426	MUC6	127	19.04.	12°16.68’	077°14.95’	17
M136-426	MUC6 DOM	127	19.04.	12°16.68’	077°14.95’	12
M136-488	BIGO II-3 C1	130	25.04.	12°16.79’	077° 15.01’	9
M136-503	BIGO I-3 C1	145	26.04.	12°18.70’	077°17.79’	10
M136-338	MUC1	165	12.04.	13°53.69’	076°30.61’	16
M136-471	BIGO I-2 C2	194	23.04.	12°21.51’	077°21.71’	7
M136-412	MUC5	243	18.04.	12°23.30’	077°24.18’	18
M136-412	MUC5 DOM	243	18.04.	12°23.30’	077°24.18’	12
M136-415	BIGO II-1 C1	243	18.04.	12°23.31’	077°24.17’	7
M136-430	BIGO I-1 C2	302	19.04.	12°24.89’	077°26.29’	8
M136-574	MUC10 **	302	01.05.	12°24.90’	077°26.29’	30
M136-342	MUC2	307	12.04.	13°57.36’	076°35.63’	16
M136-444	MUC7 *	750	20.04.	12°31.37’	077°35.00’	39
M136-543	MUC9	750	28.04.	12°31.35’	077°35.01’	14
M136-460	BIGO II-2 C1	752	21.04.	12°31.37’	077°34.99’	9
M136-409	MUC4	862	17.04.	14°02.02’	076°42.30’	8
M136-588	MUC12 ***	972	02.04.	12°34.90	077°40.34’	7
M136-545	BIGO I-4 C1	984	28.04.	12°34.88	077°40.39’	6

† Cores labelled 'DOM' were used for porewater analysis of dissolved organic matter in the onshore laboratory.
* Core for the incubation experiment at 750 m (control core plus 3 replicates).
** Two cores sectioned from this MUC, with and without a thick surface bacterial mat.
*** Two cores sectioned from this MUC deployment.

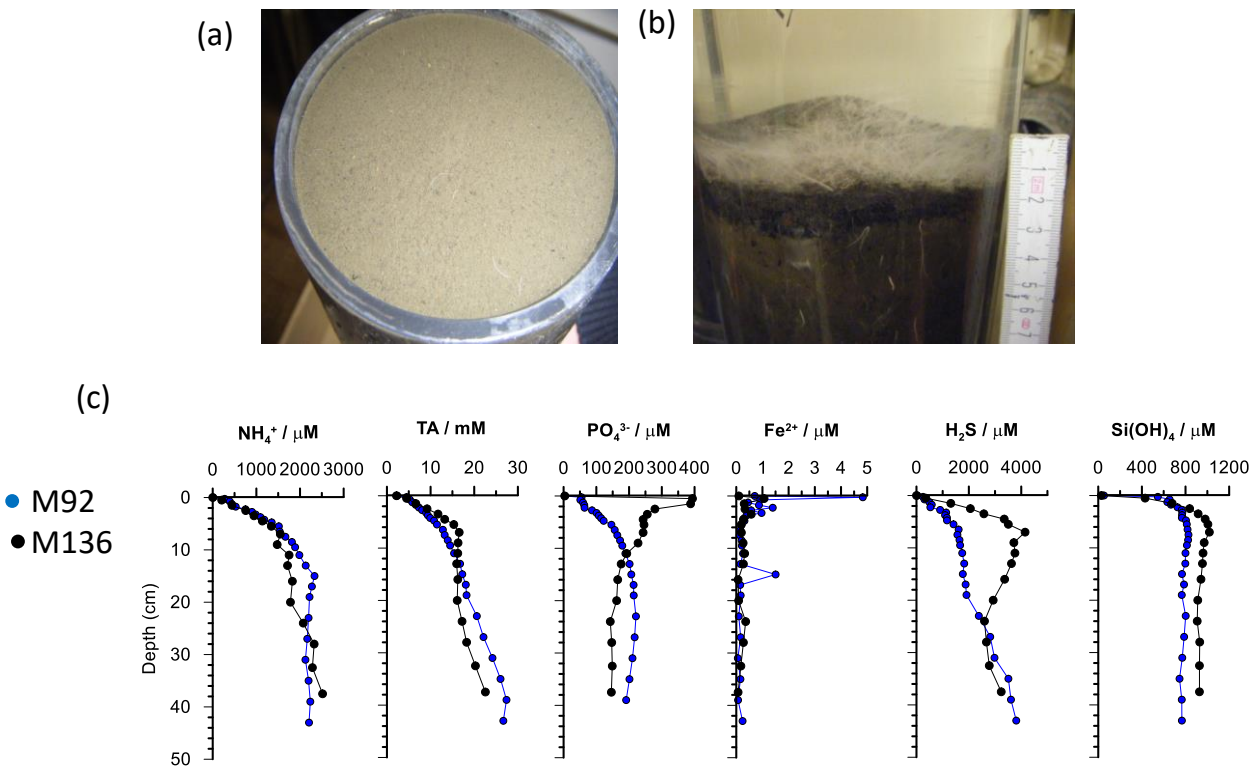

Fig. 5.7: Photographic images of surface sediments at (a) the shelf station (74 m, 483MUC8), and (b) the same station during M92 in 2013. (c) Measured concentration profiles of dissolved NH_4^+, TA, PO_4^{3-}, Fe^{2+}, H_2S, $Si(OH)_4$ in sediment porewaters sampled by the multi-corer at the shelf station (74 m, 483MUC8) compared to results from the same station during M92 (Dale et al., 2016).

5.5 Surface drifting sediment traps

(F. Le Moigne, C. Cisternas-Novoa, J. Roa)

A crucial biogeochemical mechanism in today's climate involves the transfer of carbon from the shallow to the deep ocean, the biological carbon pump (BCP). There is currently little consensus on the fate of sinking particles and the efficiency of the BCP in OMZs. Previous particles flux studies have suggested that the BCP is more efficient in suboxic zones relative to well-oxygenated waters. However, incubations performed on sinking material collected in oxic and suboxic environments showed similar remineralization rates in both conditions suggesting that suboxic conditions do not enhance the transfer of sinking organic matter through the mesopelagic zone. Moreover, the export flux of particulate nitrogen is deemed to have a strong influence of the amount of nitrogen lost through microbial processes like annamox and denitrification (Kalvelage et al., 2013). Our work aims at advancing understanding of the biogeochemistry influencing the export of organic matter into the deep ocean in tropical OMZs.

During M136, four surface tethered sediment traps (Engel et al., 2017) were successfully deployed for periods between 72 and 144 hours. Deployments dates, locations, sampling depths and parameters sampled are presented in Fig. 5.8 and Tab. 5.6. The design of the trap devices and the drifting array follows (Knauer et al., 1979), with 12 particle interceptor traps (PITs) mounted on a polyvinyl chloride (PVC) cross frame. The PITs are made of acrylic tubes with an inside diameter of 7 cm, an outside diameter of 7.6 cm and a height of 53 cm. PVC crosses with PITs were attached to a floating line, with a buoy in surface and a weight at the bottom of the

line. Prior to each deployment, PITs were filled with 1.5 L of filtered surface seawater (0.2 µm pore size cartridge) collected from the CTD at 200 m near the deployment site. A brine solution was prepared by dissolving 50 g L^{-1} sodium chloride with filtered surface seawater and subsequently filtered through a 0.2 µm cartridge to remove excess particulates. This was added at the bottom of the PITs. 20 mL of formalin was added per liter of solution (final concentration 0.74% formalin).

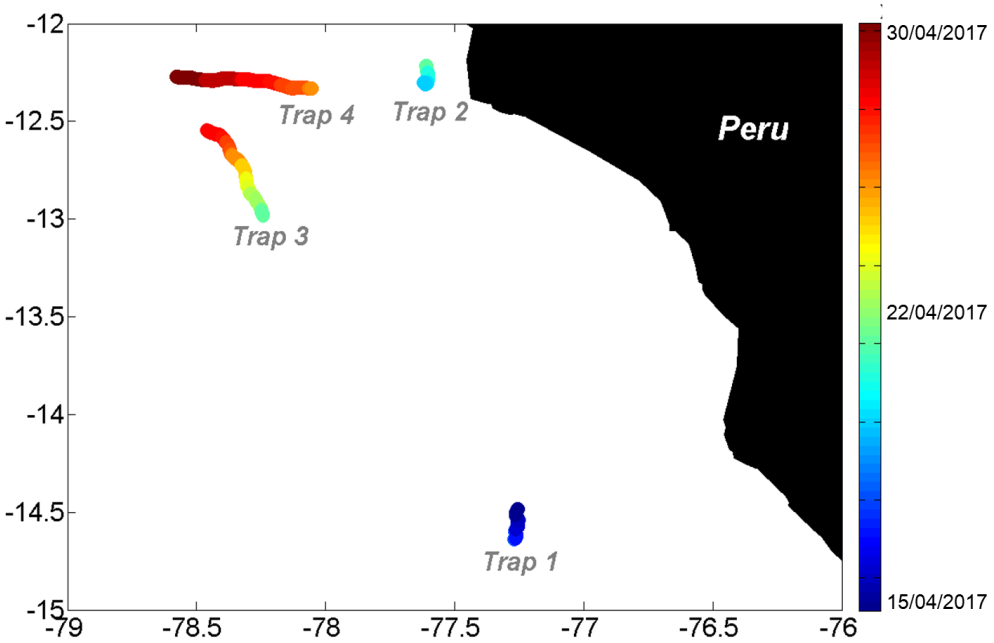

Fig. 5.8: Map of the tracks of sediment trap released and recovered during M136.

Additionally to the four trap deployments, water from the CTD was sampled at stations corresponding the trap deployments and recovery locations and also once per day when no trap recovery nor deployment occurred. The parameters sampled from the CTD and associated depths are listed in section 7.2.

Tab. 5.6: Deployments dates, depths and parameters for trap 1, 2, 3 and 4.

	Trap 1	**Trap 2**	**Trap 3**	**Trap 4**
Deployment date	Apr. 15, 16:14	Apr. 20, 00:20	Apr. 22, 15:15	Apr. 26, 20:49
Recovery date	Apr. 17, 13:27	Apr. 24, 01:15	Apr. 28, 22:32	Apr. 30, 21:02
Depths	50, 100, 150, 200, 300, 400, 500, 600m	40, 100, 150, 200, 300m	50, 75, 100, 200, 300, 400, 500, 600m	50, 100, 150, 200, 300, 400, 500, 600m
measured parameters	POC, PN, POP, mass, Chl-a, BSi, PAA, PCHO, TEP, CSP, DNA	POC, PN, POP, mass, Chl-a, BSi, PAA, PCHO, TEP, CSP, DNA	POC, PN, POP, mass, Chl-a, BSi, PAA, PCHO, TEP, CSP, DNA	POC, PN, POP, mass, Chl-a, BSi, PAA, PCHO, TEP, CSP, DNA, imaging gels

All parameters from traps and CTDs (Tab. 5.6 and section 7.2) will be analyzed following methods presented in Cisternas Novoa et al., (2015) and Engel et al. (2017). We will calculate elemental fluxes of the various trap parameters at each depth. Thereby, the concentrations of various parameters determined from the CTD stations (section 7.2) will serve as background

information for the analysis of the traps content but will also provide a general biogeochemical status of the water column. The gels for imaging used on trap 4 will be analyzed using methods presented in Laurenceau-Cornec et al. (2015) in order to obtain information on the type of particles present at each depth.

5.6 Trace metal sampling

(M. Hopwood, E. Achterberg)

5.6.1 Trace metal CTD

Trace metal (TM) sampling in the water column was planned for 4 cruises M135-M138 with the sampling procedure remaining the same on all 4 cruises. A trace metal clean sampling rosette and winch were operated from METEOR's A-frame with the winch container mounted in the central position at the stern of the ship. A pre-fabricated lab container with in-built air filtration was positioned forward and starboard of this. The trace metal clean sampling rosette was equipped with GO-FLO bottles which were stored in the trace metal clean lab container when not in use. Before trace metal (CTD-TM) stations, GO-Flo bottles were covered with protective plastic caps, bottoms and gloves over the spigots inside the clean container. They were then carried onto deck and mounted onto the trace metal sampling rosette. Immediately (maximum 5 minutes) before deployment the protective plastic was removed. Upon return to deck, gloves were immediately added to the spigots and then the GO-FLO bottles returned to the clean laboratory for sampling.

Sampling for contamination-sensitive parameters (trace metals, particles for elemental analysis, DOP, Fe(II)) was undertaken inside the clean container. Positive air pressure was maintained in the container via a continuous inward air flow, with dust particles in this air flow removed by a HEPA filter. Inside the laboratory, clean suits were worn and all labware was free from exposed metal components. N_2 gas was used to overpressure (0.2 atm) all Go-Flo bottles. O_2 samples were collected immediately after bottles were in the clean container. Sampling then proceeded around the Go-Flo bottles in the order trace metals Fe(II), isotopes, DOP, nutrients, salinity. Overall 18 TM stations were sampled with 226 dissolved trace metal samples collected and acidified for analysis in Kiel.

Trace elements:

Samples were collected in acid washed 125 mL LDPE sample bottles for dissolved (0.2 µm filter capsule) trace metal concentrations (metals: Fe, Zn, Mn, Mg, Cu, Co, Cd, Al). Samples were acidified with 180 µL concentrated (10 M) Optima grade hydrochloric acid, in batches and under a laminar flow hood, within 2 days of collection. These samples will be measured on return to GEOMAR via pre-concentration on a SeaFAST system (ESI) and subsequent analysis on an Element 2 ICP-MS (Thermo Scientific) following the method of Rapp et al. (2017). In addition to dissolved samples, 50 samples (10 depths at 5 stations) were re-filtered at 0.02 µm to determine colloidal (0.02-0.2 µm) metals.

Major nutrients and DOP/DON:

Samples were collected for dissolved macronutrients and dissolved organic phosphate (DOP) and dissolved organic nitrogen (DON) concentration analyses. 20 mL samples were collected Falcon tubes for macronutrient concentrations. 30 mL samples for DOP analysis were collected separately in acid washed HDPE bottles. DOP/DON samples were then frozen immediately in a -20°C freezer. These samples will be analysed on return to GEOMAR using a nutrient

autoanalyser following breakdown of the DOP/DON to inorganic phosphate and nitrate respectively. Macronutrients were stored refrigerated and measured onboard within 1 day of collection.

Particles

For approximately 10 depths at every CTD-TM station, 4 L of seawater as filtered through Sartorius PES 0.2 µm filters to collect sufficient particles for elemental analysis in Kiel (this volume was reduced to 0.5-2 L at coastal stations with high suspended sediment loads). Filters were mounted on plastic, acid cleaned, filter holders and attached directly to Go-Flo bottles (still under N_2) and then allowed to drain for approximately 2-3 hours. Filters were then rinsed with de-ionized water (10 mL) and frozen in a -20°C freezer. They will be digested and analysed via ICP-MS in Kiel.

Fe(II):

Fe(II) samples (unfiltered) were collected in acid cleaned 125 mL opaque HDPE bottles which were filled to overflowing and then analysed as quickly as possible within the trace metal clean container. Analysis typically commenced within 1 minute of sample collection and was always complete within 10 minutes of sample collection. A Fe(II) flow injection analysis system was assembled in the clean container using luminol chemiluminescence. A total of 50 samples were analysed abroad consisting of 5 stations along the 12 degree S section with 10 depths analysed at each station. In order to compare measured Fe(II) concentrations with anticipated Fe(II) oxidation rates, water samples were also retained for: pH (unfiltered water retained in 250 mL glass stoppered bottles preserved with 0.5 mL saturated $HgCl_2$ solution) which will be determined by measurement of dissolved inorganic carbon and total alkalinity in Kiel, total organic carbon (unfiltered water retained in 30 mL glass bottles and acidifed to pH 2 by addition of trace metal grade HCl), and Fe-L analysis (500 mL 0.2 µm filtered water frozen at -20°C).

Cd isotopes:

Samples were collected in acid washed 1-8 L LDPE bottles for dissolved (0.2 µm filter capsule) Cd isotopic analysis. These samples were then stored sealed in plastic bags, acidified to pH <2 by addition of optima grade HCl within 2 days of collection and will be analysed upon return to Kiel. A total of 48 samples were kept for Cd isotopes, collected from 4 stations along the 12 S section.

5.6.2 Underway tow fish measurements

Surface (~2-3 m depth) seawater was sampled from a custom-built towed-fish via acid washed 1 cm diameter tubing with suction provided by a peristaltic pump. Water was pumped directly into the purpose-built clean air laboratory container. 36 samples collected during M136 and were retained for dissolved macronutrient (nitrate, nitrite, phosphate, silicate) concentrations, trace element concentrations, and (for select sections only) Cd isotopes (H_2O_2). Sample collection for this suite of measurements was carried out with a preference for sampling just before or after (~10-15 minutes) a CTD-TM station.

5.7 Microbial N transformations: the importance of microniches

(L. Bristow, C. Karthäuser, G. Lavik)

During M136 an extensive program was undertaken to examine the role of particles in the microbial nitrogen cycle relative to the overall rates. Sinking of aggregated particles is considered to be one of the main mechanisms of organic matter export from the surface ocean to

deeper water layers. These aggregated particles are characterized by strong chemical gradients with substrate availabilities very different to ambient waters (i.e. oxygen, nutrients, organic carbon) offering microniches for microorganisms. Thus, microbial processes associated with particle related microniches may strongly regulate microbial diversity and function within low oxygen regions.

Water and single aggregate samples were collected from the OMZ along the 12 and 14°S transects. The samples were collected with a CTD rosette (water samples), a marine snow catcher (single aggregates) and a benthic boundary layer sampler (BBL sampler; both water samples and single aggregates). Water samples (total 11 stations; 3 to 6 depths per CTD or BBL sampler deployment) were amended with different combinations of ^{15}N and ^{14}N labeled substrates to determine rates of microbial nitrogen transformations (anammox, denitrification, nitrate reduction, ammonia oxidation, nitrite oxidation, DNRA). At 5 of these stations, rates were conducted in three size fractions (bulk, < 10 µm and < 1.6 µm) to assess which microbial nitrogen cycling processes are particle associated and how this varies across chemical gradients.

Single aggregates were collected at 9 stations from the marine snow catcher or BBL sampler. These were incubated with the same substrates as the water samples but incubated under constant rotation, to mimic sinking. In addition, single aggregates were collected at each station for the determination of carbon content, visualization and characterization of the microbial community, elemental composition and sinking velocity.

Along the M136 cruise track, a total of 34 nitrogen fixation and primary productivity experiments ($^{15}N_2$ and ^{13}DIC additions) were conducted across 12 stations, capturing gradients in both oxygen and fluorescence. In addition, at 9 of these stations three depths across the upper oxycline were sampled for the determination of oxygen consumption rates, using $^{18}O_2$. Alongside these rate determination experiments (and those mentioned above), samples were collected to enable characterization of the microbial community DNA / RNA (sampled for Martin Fischer, CAU Kiel; 165 samples), FISH (fluorescence insitu hybridization; 213 samples) and for the determination of single cell rates, nanoSIMS (nanometer-scale secondary ion mass spectrometry) in different size fractions.

On the return of the samples to MPI Bremen, microbial nitrogen transformation rates will be determined by GC-IRMS in both water and single aggregate incubation experiments. This will allow us to determine the partitioning of nitrogen loss processes (anammox and denitrification) and the processes supplying the substrates for these processes (namely nitrate reduction, ammonia oxidation and nitrite oxidation) between the free living (< 1.6 µm) and particle associated fractions. These rates will be correlated with single aggregate properties such as size, carbon content, and sinking velocity. Analysis of the microbial community in the different size fractions (Martin Fischer, CAU Kiel), alongside FISH and nanoSIMS analyses on slices of individual aggregates will allow us to assess which microorganisms are the key players in each fraction and if particle associated, their location within an aggregate (surface versus inside). Taken together, these results will be correlated with the primary productivity data and scaled up in collaboration with other groups onboard (UVP and sediment trap data), allowing us to assess the contribution of particle associated microniches to microbial nitrogen cycling in low oxygen regions.

5.8 Evaluation of the biological carbon pump efficiency using the ^{234}Th isotopes

(R.C. Xie, E. Achterberg)

The radionuclide thorium ^{234}Th, with a half-life of 24.1 days, is constantly produced by the decay of its parent uranium ^{238}U. While uranium is highly soluble and conservative in oxygenated waters, thorium is very particle reactive. The deficit of ^{234}Th in the upper water column thus is generally used to quantify export fluxes from the euphotic zone to the deeper ocean. Conversely, as particles remineralize below the photic zone, ^{234}Th is released back to the water column; thus the vertical profiles of ^{234}Th allow the estimation of remineralization rates. With information on the particulate carbon to ^{234}Th (POC/^{234}Th) ratios from sinking particles, or any chemical parameters of which the ratio to ^{234}Th can be determined, one can estimate the export fluxes of carbon (or nitrogen, phosphorus, or trace metals). When compared with data on primary production, these estimates on carbon export allow the evaluation of the efficiency of the biological carbon pump.

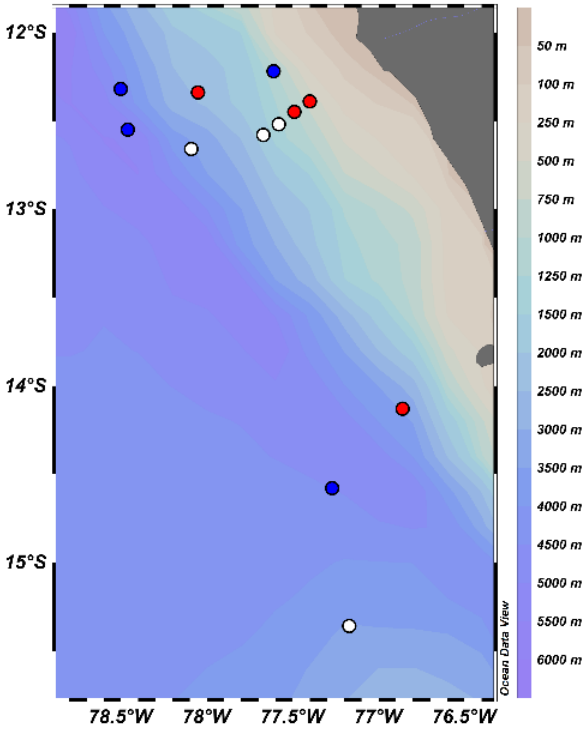

Fig. 5.9: Location of ^{234}Th stations during M136. Red circles indicate stand-alone pump system deployment locations, blue circles mark location of stand-alone pump system deployments combined with sediment trap recoveries, white circles mark CTD sampling stations only.

During M136, unfiltered seawater samples (4L each) for total ^{234}Th activities, including both dissolved and particulate phases, were collected from Niskin bottles mounted on a traditional CTD at 13 stations (Fig. 5.9) along the 12˚S and 14˚S transects. Higher-resolution sampling was performed at the upper 200 m where most of the biological activities occur; additional depths were sampled down to 1500 m, or 100 m above the seafloor. Two stations at 2000 m (bottom depth) and 400 m were sampled twice to look at the temporal variability of total ^{234}Th. Filtered (0.45 Acropak® polycarbonate membrane) seawater (15 ml) for uranium concentrations was sampled at the same Niskin bottles for ^{234}Th.

Suspended (1 – 50 µm on polycarbonate membranes) and sinking particulates (> 50 µm on Nitex mesh) were collected using the Challenger stand-alone pump system (SAPS) (Fig. 5.9) deployed with a plastic cable. Four of the SAPS stations were sampled at sites where sediment

traps were recovered, to investigate the agreement and differences in carbon export estimated from both methods.

The chemical separation of thorium from seawater on board followed Pike et al. (2005). Thorium was co-precipitated with MnO_2 and filtered onto 25 mm QMA filters. These precipitates were dried in an oven at 55˚C.

For the sinking particles, each filter was evenly split in halves using a ceramic knife. One half of each filter was folded and frozen at -20˚C for trace metal analysis back in home laboratory, while the other half was split equally into four quarters. Particles from each quarter were re-suspended in filtered seawater, and re-filtered onto (1) pre-combusted QMA filters for Th, POC, and PON; (2) pre-combusted GFF filters for PIP; (3) pre-combusted GFF filters for POP; and (4) GFF filters for pigment. Pigment samples were stored at the -80˚C fridge/container until analysis at home laboratory. Filters with samples of Th, POC, PON, PIP, and POP were dried in an oven at 55˚C. Filters of total and particulate Th were mounted onto the Risø sample holders, and the activities of ^{234}Th were counted on the Risø low-level beta GM multicounter. Filters with suspended particles for trace metal were folded and stored at -20˚C until analysis at home laboratory.

5.9 Dissolved organic matter sampling

(Marie Maßmig, Tania Klüver, Jon Roa, Anja Engel)

To study the influence of oxygen concentrations on the bacterial growth and degradation of organic matter, seawater samples for the analysis of dissolved organic matter concentration, cell abundance, extracellular enzyme rates and bacterial biomass production were collected. Altogether, samples were taken at 20 CTD stations from 4 to 11 different depths along the northern (11°S) and southern (13°S) transect - including the stations of sediment trap deployment and recovery (Fig. 5.10). The different depths covered a broad range of *in-situ* oxygen concentrations crossing the upper and lower oxicline (Table 5.7).

Organic matter hydrolysis by extracellular enzymes is the key step in bacterial degradation of organic matter. The rates of the three abundant extracellular enzymes leucine aminopeptidase, ß glucosidase and alkaline phosphatase were measured with different concentrations of fluorescent substrate analogues to achieve Michalis Menten kinetics according to Hoppe (1983). Furthermore, bacterial biomass production, as estimate for bacterial growth, was measured after Kirchman et al. (1985) by the bacterial uptake of radioactive labelled leucine (^{3}H). Both parameters were incubated under two oxygen levels (oxic and anoxic conditions) at 13°C. Since enzymes are known to be pH sensitive also the pH was measured at all depth. Rate measurements will be compared to bacterial cell abundances (determined by flow cytometry after Gasol and del Giorgio (2000)). In order to describe the *in situ* substrate availability for bacteria, samples for dissolved organic carbon concentrations (DOC), as well as concentrations and composition of dissolved amino acids (DAA) and dissolved high molecular weight carbohydrates (DCHO) were taken, filtered and stored at +4°C or -20°C respectively. DOC will be analyzed with a high temperature combustion method after Sugimura and Suzuki (1988) and Engel and Galgani (2016). For analyzes of DAA the high performance liquid chromatography method after Lindroth and Mopper (1979) will be applied and DCHO will be analyzed after Engel and Händel (2011). Additionally, dissolved organic phosphate (DOP) was sampled at selected depths and will be determined after Grasshof (1999). Samples for bacterial abundances,

DOC, DAA, DCHO and DOP were shipped frozen or cooled to the home laboratory at GEOMAR and will be analyzed within the next six month. Data will be available in OSIS within one year.

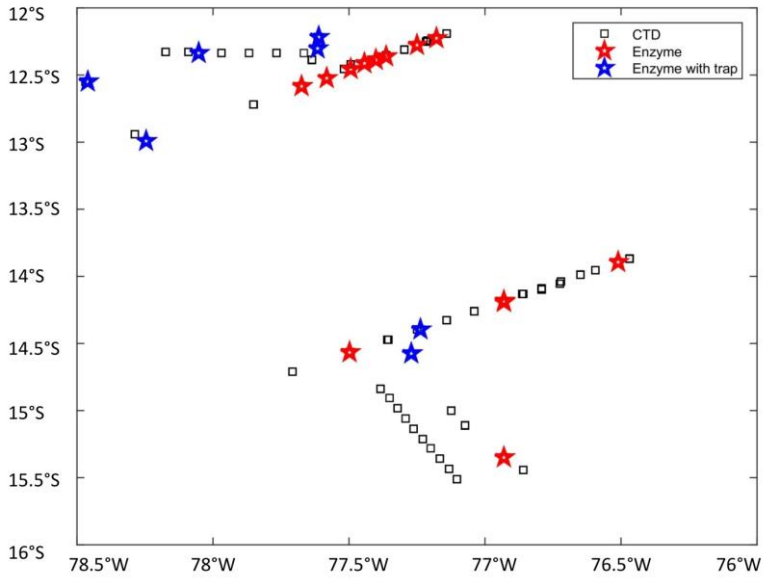

Fig.5.10: Map of all sampled CTD profiles during M136. The blue and red stars indicate sampled stations for the parameters listed in Tab. 5.7.

Table 5.7: CTD profiles and depths sampled for dissolved organic carbon (DOC), dissolved high molecular weight carbohydrates (DCHO), dissolved amino acids (DAA), cell abundance, extracellular enzyme rates (Enzymes), pH and bacterial biomass production (BBP). Selected depths were additionally sampled for dissolved organic phosphorous (DOP).

METEOR station	CTD profile	Sampling depth in meters of	
		cell abundance (bacteria & phytoplankton), DOC, DAA, DCHO, BBP, Enzymes, pH	DOP
339	2	4, 10, 15, 19, 30, 39, 50, 69, 99, 128, 159	4,10,19, 50, 99
358	10	5, 14, 29, 49, 81, 101, 123, 199, 399, 599, 1992	5, 49, 101, 199, 599
368	13	5, 49, 89, 99, 148, 198, 299, 399, 499, 599, 1998	5, 49, 99, 499, 599
374	16	9, 35, 69, 99 *	
393	32	5, 18, 40, 58, 99, 109, 118, 130, 199, 300, 405	5, 58, 109, 130, 199
402	39	3, 19, 49, 78, 99, 147, 198, 299, 398, 499, 600	3, 49, 99, 198, 398
422	43	3, 19, 39, 55, 65, 90, 98, 199, 238	
432	46	4, 9, 38, 99, 147	4, 9, 38, 99, 147
435	47	4, 9, 13, 19, 23, 28, 43, 48, 58	4, 13, 23, 43, 58
445	50	4, 29, 39, 49, 59, 79, 89, 98, 147, 597, 745	29, 49, 98, 147, 745
456	55	3, 18 50, 99, 124, 149, 174, 224, 272, 300	3, 18 50, 124, 272
467	59	4, 29, 49, 60, 74, 99, 196, 296, 396, 599, 800	4, 49, 74, 99, 599
472	61	4, 19, 38, 58, 83, 100, 149, 198, 298	4, 38, 58, 83, 298
480	63	4, 19, 24, 28, 49	4, 19, 24, 28, 49
491	66	3, 6, 18, 27, 39, 48, 58, 68, 79, 98, 128	
508	71	4, 18, 28, 39, 49, 59, 73, 199	4, 28, 39, 59, 73
516	74	9, 50, 75, 99, 148, 157, 199, 299, 398, 499, 599	9, 75, 99, 148, 157
532	82	4, 20, 25, 30, 39, 49, 59, 72	20, 30, 39, 49, 59
547	87	9, 39, 47, 73, 99, 108, 198, 299, 398, 499, 593	9, 47, 73, 108, 593
559	91	4, 28, 49, 68, 78, 99, 195, 393, 448, 498, 598,	4, 49, 78, 448, 498
567	92	5, 30, 50, 70, 100, 150, 200, 300, 400, 500, 600	5, 70, 100, 150, 500

* DOC, DAA, DCHO were not measured at this station

Since oxygen has a higher electron potential than alternative electron acceptors and thus provides more energy to the microbial community as nitrate, we expect higher growth and degradation rates under oxic conditions. However former studies, did not find any oxygen dependence of bacterial biomass production as well as enzyme activity (Pantoja et al. 2009). Here we collected more data to find possible statistical correlations and dependencies between oxygen concentrations and bacterial biomass production as well as extracellular enzyme rates. As enzymes in the field are known to be inversely correlated with their respective nutrient concentrations as it is described for depth profiles of peptidase and dissolved inorganic nitrogen (Nausch and Nausch, 2000), or in experiments with alkaline phosphatase and phosphorus forms (Torriani 1960), we also expect lower enzyme rates at higher nutrient concentrations. The preliminary analysis of the measured extracellular enzyme rates and bacterial biomass production showed differences between oxic and anoxic incubations. Furthermore, we observed higher rates at the more coastal (and therefore nutrient-rich) stations decreasing with depth

6 Ship's meteorological station

(H. Rentsch, A. Raeke)

R/V METEOR left port Callao in the afternoon on April 11, 2017 for its voyage M136. The ship sailed along the edge of a dynamical high pressure system of 1035 hPa situated at 35°S and 100°W. A cloudy sky and southerly winds 3 to 4 Beaufort (Bft.) were dominant until the first CTD-station taken on the following day.

During most of the expedition, south-southeasterly trade winds of 4-5 Bft (more than 80% of the time) prevailed and we experienced a sea state of 2 to 2.5 m (more than 60%). Heights of the wind waves were predominately below 1.5 m. After April 17 for a period of about 5 days, southeasterly winds decreased to 2-3 Bft. and sea state decreased to about 1 m. During April 15, a 3-day period from April 22 to 24 and during May 2, increase southeasterly winds of 5 to 6 Bft and sea state (swell around 2 m, 7-11 s) having wave heights of about 2.5 m were observed.

Convective processes, reaching upper levels of troposphere, did not occur during the survey. The reason for that was a settled inversion of temperature of the trade-wind zone together with the cold waters of the Humboldt Current. Thus, the elevated temperatures sufficient to start convection in the troposphere were never reached. Instead, cloudiness during the cruise was often characterized by strati form clouds below 2.5 km height and occasionally some clouds in upper levels (above 700 hPa-level) in an average of 4 to 7 parts from 8. The meteorological office on board visited some light showers. However, the total sum of precipitation measured during the cruise did not exceed 0.1 mm.

During the cruise, sea surface temperature (SST) varied between 17°C and 22°C. Likewise, temperatures of air above the surface were between 18°C and 22°C. Variability of the surface wave- and wind field were caused primarily by the ship position relative to the coastal upwelling SST front and changes of the horizontal pressure gradient of the steering Subtropical high southerly of our working areas. Furthermore, the daily course of atmospheric turbulence, orographic effect of the coastline and the proximity of the vessels to little islands caused wind variability.

On Wednesday, May 3 2017 in the morning, RV METEOR reached the port of Callao together with temperatures nearby 20°C, weak southeasterly winds and a nearly calmed sea.

7 Station list M136

7.1 Overall station list

Station No.		Date	Gear	Time	Latitude	Longitude	Water Depth	Remarks/Recovery
METEOR (M136-)	GEOMAR	2017		[UTC]	[°S]	[°W]	[m]	
335-1	RC 1	12.04.	Rapid Cast	00:33	12° 43.36'	076° 51.83'	134.3	
336-1	CTD 1	12.04.	CTD/RO	13:07	13° 51.90'	076° 28.10'	88.4	CTD Station (80 m, bottom)
337-1	MSS 1	12.04.	MSS	13:44	13° 51.92'	076° 28.10'	87.3	
338-1	MUC 1	12.04.	TV-MUC	15:20	13° 53.69'	076° 30.65'	165.6	Multicorer 160 m
339-1	CTD 2	12.04.	CTD/RO	16:01	13° 53.64'	076° 30.61'	166.0	CTD Station (160 m, bottom)
340-1	MSS 2	12.04.	MSS	17:15	13° 53.81'	076° 30.64'	163.7	
341-1	CTD 3	12.04.	CTD/RO	18:23	13° 53.70'	076° 30.62'	164.2	CTD Station (160 m, bottom)
342-1	MUC 2	12.04.	TV-MUC	20:15	13° 57.36'	076° 35.63'	307.4	Multicorer 300 m
343-1	KPO1183	12.04.	Mooring	23:37	13° 58.414’	076° 47.942’	990.0	Mooring deployment
343-2	RC 2	13.04.	Rapid Cast	00:00	13° 58.43'	076° 47.52'	956.8	
344-1	CTD 4	13.04.	CTD/RO	01:21	13° 57.39'	076° 35.64'	305.5	CTD Station (300 m, bottom)
345-1	MSS 3	13.04.	MSS	02:14	13° 57.40'	076° 35.61'	306.4	
346-1	CTD 5	13.04.	CTD	04:15	13° 59.37'	076° 39.00'	505.6	CTD Station (500 m, bottom)
347-1	MSS 4	13.04.	MSS	05:09	13° 59.38'	076° 39.00'	505.1	
348-1	CTD 6	13.04.	CTD/RO	06:45	14° 02.36'	076° 43.24'	1051.0	CTD Station (1050 m,
349-1	MSS 5	13.04.	MSS	07:56	14° 02.38'	076° 43.25'	1056.3	
350-1	CTD 7	13.04.	CTD/RO	08:56	14° 03.41'	076° 43.58'	1173.2	CTD Station (200 m)
351-1	CTD 8	13.04.	CTD/RO	10:09	14° 05.15'	076° 47.47'	1903.5	CTD Station (1950 m,
352-1	MSS 6	13.04.	MSS	11:56	14° 05.99'	076° 47.97'	1990.5	
353-1	CTD 9	13.04.	CTD/RO	13:37	14° 08.02'	076° 51.67'	2073.9	CTD Station (2000 m)
354-1	CTD-TM 49	13.04.	CTD-TM	15:19	14° 08.02'	076° 51.67'	2312.7	
355-1	MSS 7	13.04.	MSS	17:10	14° 08.49'	076° 51.10'	2355.6	
356-1	ISP 1	13.04.	In-situ pumps	18:14	14° 08.06'	076° 51.77'	2315.0	Pumps at 30 m, 100 m, 400 m depth
357-1	MSS 8	13.04.	MSS	21:23	14° 09.79'	076° 56.32'	2984.8	
358-1	CTD 10	13.04.	CTD/RO	22:25	14° 10.90'	076° 55.86'	3019.9	CTD Station (2000 m)
359-1	MSS 9	14.04.	MSS	00:37	14° 14.13'	077° 01.99'	3824.3	
360-1	CTD 11	14.04.	CTD	02:10	14° 15.56'	077° 02.29'	3903.1	CTD Station (2000 m)
361-1	MSS 10	14.04.	MSS	05:06	14° 18.11'	077° 08.29'	4802.0	
362-1	CTD 12	14.04.	CTD/RO	06:06	14° 19.57'	077° 08.56'	4799.2	CTD Station (2000 m)
363-1	RC 3	14.04.	Rapid Cast	07:28	14° 19.58'	077° 08.56'	4795.3	
364-1	MSS 11	14.04.	MSS	08:17	14° 22.17'	077° 14.77'	5148.2	
365-1	SC 1	14.04.	Snow Catcher	11:02	14° 23.83'	077° 14.85'	5103.5	Snow catcher closed at 100 m depth
366-1	CTD-TM 50	14.04.	CTD-TM	11:53	14° 23.83'	077° 14.86'	4994.4	
367-1	Trap 1	14.04.	Sediment trap	16:07	14° 23.85'	077° 14.83'	5127.7	Deployment of drifting sediment trap
368-1	CTD 13	14.04.	CTD/RO	17:00	14° 23.93'	077° 14.33'	5150.9	CTD Station (2000 m)
369-1	RC 4	14.04.	Rapid Cast	18:23	14° 23.94'	077° 14.35'	5147.3	
370-1	CTD 14	14.04.	CTD/RO	19:17	14° 28.13'	077° 21.31'	4685.2	CTD Station (2000 m)
371-1	SC 2	14.04.	Snow Catcher	22:52	14° 33.90'	077° 29.76'	4422.7	Snow catcher closed at 130 m depth
372-1	CTD 15	14.04.	CTD/RO	23:23	14° 33.90'	077° 29.77'	4426.2	CTD Station (2000 m)
373-1	MSS 12	15.04.	MSS	00:54	14° 33.97'	077° 29.73'	4424.7	
374-1	CTD 16	15.04.	CTD/RO	02:16	14° 33.90'	077° 29.79'	4421.6	CTD Station (400 m)
375-1	CTD 17	15.04.	CTD/RO	04:43	14° 42.47'	077° 42.43'	4196.4	CTD Station (2000 m)
376-1	RC 5	15.04.	Rapid Cast	06:10	14° 42.61'	077° 42.40'	4192.2	
377-1	CTD-TM 51	15.04.	CTD-TM	13:27	15° 36.42'	077° 03.46'	2881.0	

378-1	CTD 18	15.04.	CTD/RO	15:12	15° 30.72'	077° 06.14'	2926.2	CTD Station (200 m)
379-1	CTD 19	15.04.	CTD/RO	16:18	15° 26.15'	077° 08.04'	2972.8	CTD Station (200 m)
380-1	CTD 20	15.04.	CTD/RO	17:23	15° 21.64'	077° 10.00'	3062.1	CTD Station (600 m)
381-1	CTD 21	15.04.	CTD/RO	18:46	15° 17.05'	077° 11.83'	3228.2	CTD Station (200 m)
382-1	CTD 22	15.04.	CTD/RO	19:45	15° 12.63'	077° 13.71'	3402.4	CTD Station (200 m)
383-1	CTD 23	15.04.	CTD/RO	20:48	15° 07.95'	077° 15.64'	3447.4	CTD Station (200 m)
384-1	CTD 24	15.04.	CTD/RO	21:50	15° 03.53'	077° 17.50'	3778.7	CTD Station (200 m)
385-1	CTD 25	15.04.	CTD/RO	22:55	14° 59.05'	077° 19.29'	3830.8	CTD Station (200 m)
386-1	CTD 26	15.04.	CTD/RO	23:59	14° 54.56'	077° 21.15'	3835.2	CTD Station (200 m)
387-1	CTD 27	16.04.	CTD/RO	00:58	14° 50.22'	077° 23.01'	4085.1	CTD Station (200 m)
388-1	CTD 28	16.04.	CTD/RO	02:01	14° 45.47'	077° 24.94'	4186.7	CTD Station (200 m)
389-1	CTD 29	16.04.	CTD/RO	03:04	14° 40.89'	077° 26.87'	4306.9	CTD Station (200 m)
390-1	CTD 30	16.04.	CTD/RO	04:18	14° 33.87'	077° 29.73'	4424.2	CTD Station (200 m)
391-1	RC 6	16.04.	Rapid Cast	04:58	14° 34.20'	077° 29.54'	4418.8	
392-1	CTD 31	16.04.	CTD/RO	12:09	15° 26.80'	076° 51.64'	2973.8	CTD Station (400 m)
393-1	CTD 32	16.04.	CTD/RO	13:35	15° 21.00'	076° 55.82'	3199.7	CTD Station (400 m)
394-1	CTD-TM 52	16.04.	CTD-TM	14:30	15° 21.00'	076° 55.81'	3201.5	
395-1	CTD 33	16.04.	CTD/RO	15:23	15° 21.05'	076° 55.85'	3199.5	CTD Station (400 m)
396-1	CTD 34	16.04.	CTD/RO	17:46	15° 06.50'	077° 04.29'	3532.6	CTD Station (1000 m)
397-1	CTD 35	16.04.	CTD/RO	19:34	15° 00.01'	077° 07.50'	3763.5	CTD Station (400 m)
398-1	CTD 36	16.04.	CTD/RO	21:35	14° 47.65'	077° 11.87'	4210.3	CTD Station (400 m)
399-1	CTD 37	16.04.	CTD/RO	23:09	14° 37.96'	077° 13.52'	4495.5	CTD Station (400 m)
400-1	CTD 38	17.04.	CTD/RO	01:12	14° 23.80'	077° 14.91'	5128.3	CTD Station (400 m)
401-1	ISP 2	17.04.	In-situ pumps	03:37	14° 34.55'	077° 16.24'	4454.5	Pumps at 30 m, 100 m, 200 m, 400 m, 590 m depth
402-1	CTD 39	17.04.	CTD/RO	06:29	14° 34.55'	077° 16.24'	4456.7	CTD Station (600 m)
403-1	CTD-TM 53	17.04.	CTD-TM	07:20	14° 34.55'	077° 16.24'	4592.8	
404-1	CTD 40	17.04.	CTD/RO	08:00	14° 34.58'	077° 16.30'	4571.6	CTD Station (400 m)
405-1	SC 3	17.04.	Snow Catcher	10:11	14° 34.70'	077° 16.30'	4569.2	Snow catcher closed at 140 m depth
406-1	Trap 1	17.04.	Sediment trap	13:00	14° 37.99'	077° 16.03'	4506.6	Recovery drifiting sediment trap
407-1	RC 7	17.04.	Rapid Cast	18:16	14° 19.18'	076° 58.54'	4001.9	
408-1	MUC 3	17.04.	TV-MUC	21:05	14° 02.01'	076° 42.30'	864.5	Multicorer 800 m, failed
409-1	MUC 4	17.04.	TV-MUC	21:52	14° 02.02'	076° 42.30'	864.3	Multicorer 800 m
410-1	GLI 1	17.04.	GLIDER	23:17	13° 58.19'	076° 38.99'	480.5	Recovery Glider IFM12
411-1	GLI 2	18.04.	GLIDER	05:53	13° 40.01'	077° 40.56'	4457.2	Recovery Glider IFM09
412-1	MUC 5	18.04.	TV-MUC	13:48	12° 23.30'	077° 24.18'	242.0	Multicorer 240 m
413-1	CTD-TM 54	18.04.	CTD-TM	14:20	12° 23.30'	077° 24.18'	242.4	
414-1	KPO1181	18.04.	Mooring	17:00	12° 21.91'	077° 21.82'	199.2	Mooring deployment failed due to lost anchor weight
415-1	BIGO II-1	18.04.	BIGO	20:27	12° 23.31'	077° 24.17'	242.8	BIGO deployment
416-1	KPO1181	18.04.	Mooring	21:30	12° 22.38'	077° 20.90'	197.1	Recovery after failed deployment
	CTD 41	19.04.	CTD/RO	03:05	12° 24.90'	077° 26.26'	301.3	CTD Station (300 m, bottom)
418-1	MSS 13	19.04.	MSS	03:53	12° 24.97'	077° 26.26'	303.2	
419-1	MSS 14	19.04.	MSS	05:39	12° 22.54'	077° 25.17'	245.1	
420-1	CTD 42	19.04.	CTD/RO	06:23	12° 23.32'	077° 25.05'	255.4	CTD Station (250 m, bottom)
421-1	MSS 15	19.04.	MSS	07:05	12° 22.55'	077° 24.21'	228.0	
422-1	CTD 43	19.04.	CTD/RO	07:52	12° 23.31'	077° 24.18'	242.1	CTD Station (240 m, bottom)
423-1	CTD 44	19.04.	CTD/RO	09:12	12° 23.31'	077° 24.18'	241.5	CTD Station (240 m, bottom)
424-1	SC 4	19.04.	Snow Catcher	11:08	12° 23.30'	077° 23.98'	239.0	Snow catcher closed at 120 m depth
425-1	KPO1181	19.04.	Mooring	12:38	12° 22.288’	077° 21.779’	203.0	Mooring deployment
426-1	MUC 6	19.04.	TV-MUC	13:59	12° 16.68'	077° 14.95'	127.4	Multicorer 126 m

427-1	CTD-TM 55	19.04.	CTD-TM	16:29	12° 23.31'	077° 24.09'	242.2	
428-1	CTD 45	19.04.	CTD/RO	16:45	12° 23.31'	077° 24.09'	240.7	CTD Station (240 m, bottom)
429-1	ISP 3	19.04.	In-situ pumps	17:50	12° 23.31'	077° 24.09'	240.7	Pumps at 30 m, 80 m, 100 m, 200 m depth
430-1	BIGO I-1	19.04.	BIGO	20:59	12° 24.89'	077° 26.29'	302.8	BIGO deployment
431-1	Trap 2	20.04.	Sediment trap	00:20	12° 17.99'	077° 37.31'	471.6	Deployment drifting sediment trap
432-1	CTD 46	20.04.	CTD/RO	00:57	12° 18.24'	077° 36.96'	473.3	CTD Station (470 m, bottom)
433-1	RC 8	20.04.	Rapid Cast	01:57	12° 18.18'	077° 35.70'	503.6	
434-1	MSS 16	20.04.	MSS	04:02	12° 15.81'	077° 15.14'	128.9	
435-1	CTD 47	20.04.	CTD/RO	05:03	12° 16.71'	077° 14.95'	130.0	CTD Station (125m, bottom)
436-1	MSS 17	20.04.	MSS	06:25	12° 20.55'	077° 21.74'	186.4	
437-1	CTD 48	20.04.	CTD/RO	07:36	12° 21.41'	077° 21.85'	195.5	CTD Station (190 m, bottom)
438-1	MSS 18	20.04.	MSS	08:24	12° 22.55'	077° 23.54'	223.9	
439-1	CTD 49	20.04.	CTD/RO	10:04	12° 23.28'	077° 24.13'	243.2	CTD Station (240 m, bottom)
440-1	BIGO II-1	20.04.	BIGO	13:26	12° 23.13'	077° 24.20'	241.8	BIGO recovery
441-1	BWS 1	20.04.	BWS	15:15	12° 23.31'	077° 24.18'	242.8	
442-1	GLI 3	20.04.	GLIDER	17:40	12° 31.38'	077° 34.98'	750.4	Deployment Glider IFM12
443-1	CTD-TM 56	20.04.	CTD-TM	18:30	12° 31.37'	077° 34.98'	749.7	
444-1	MUC 7	20.04.	TV-MUC	19:46	12° 31.37'	077° 35.00'	751.9	Multicorer 750 m
445-1	CTD 50	20.04.	CTD/RO	20:24	12° 31.37'	077° 35.00'	751.9	CTD Station (750 m, bottom)
446-1	CTD 51	20.04.	CTD/RO	22:06	12° 31.37'	077° 35.00'	750.0	CTD Station (200 m)
447-1	MSS 19	20.04.	MSS	23:20	12° 26.50'	077° 30.76'	417.4	
447-1	MSS 20	21.04.	MSS	00:24	12° 27.58'	077° 31.00'	478.1	
448-1	CTD 52	21.04.	CTD/RO	02:26	12° 27.57'	077° 31.02'	444.0	CTD Station (440 m, bottom)
449-1	MSS 21	21.04.	MSS	03:35	12° 25.32'	077° 29.53'	358.5	
450-1	CTD 53	21.04.	CTD/RO	05:06	12° 27.17'	077° 29.55'	405.7	CTD Station (400 m)
451-1	MSS 22	21.04.	MSS	06:23	12° 22.97'	077° 25.56'	258.5	
452-1	CTD 54	21.04.	CTD/RO	08:39	12° 24.90'	077° 26.28'	302.5	CTD Station (300 m, bottom)
453-1	SC 5	21.04.	Snow catcher	09:36	12° 24.90'	077° 26.28'	302.0	Snow catcher closed at 130 m depth
454-1	KPO1180	21.04.	Mooring	14:20	12° 25.652’	077° 25.658’	301.0	Mooring deployment
455-1	BIGO I-1	21.04.	BIGO	15:23	12° 24.77'	077° 26.44'	304.2	BIGO recovery
456-1	CTD 55	21.04.	CTD/RO	15:52	12° 24.82'	077° 26.55'	306.2	CTD Station (300 m, bottom),
457-1	CTD-TM 57	21.04.	CTD-TM	17:41	12° 27.18'	077° 29.50'	438.3	
458-1	CTD 56	21.04.	CTD/RO	18:27	12° 27.14'	077° 29.63'	406.7	CTD Station (350 m, bottom)
459-1	ISP 4	21.04.	In-situ pumps	19:11	12° 27.14'	077° 29.63'	407.6	Pumps in 30 m, 80 m, 150 m, 300 m depth
460-1	BIGO II-2	21.04.	BIGO	22:55	12° 31.35'	077° 34.99'	748.2	BIGO deployment
461-1	CTD 57	21.04.	CTD/RO	23:31	12° 31.35'	077° 34.99'	746.8	CTD Station (740 m, bottom)
462-1	MSS 23	22.04.	MSS	01:03	12° 31.39'	077° 35.04'	753.9	
463-1	CTD 58	22.04.	CTD/RO	04:06	12° 43.32'	077° 51.01'	2092.8	CTD Station (2000 m)
464-1	MSS 24	22.04.	MSS	06:14	12° 43.36'	077° 51.01'	2150.7	
465-1	CTD-TM 58	22.04.	CTD-TM	10:30	12° 59.12'	078° 13.81'	5259.2	
466-1	Trap 3	22.04.	Sediment trap	15:12	12° 58.94'	078° 14.45'	5296.3	Deployment drifting sediment trap
467-1	CTD 59	22.04.	CTD/RO	15:40	12° 59.25'	078° 14.82'	5401.0	CTD Station (800 m)
468-1	CTD 60	22.04.	CTD/RO	17:27	12° 56.40'	078° 17.36'	5821.9	CTD Station (5820 m,
469-1	BIGO II-2	23.04.	BIGO	14:35	12° 31.14'	077° 35.23'	753.9	BIGO recovery
470-1	GLI 4	23.04.	GLIDER	19:00	12° 21.51'	077° 21.71'	194.2	Deployment Glider IFM07
471-1	BIGO I-2	23.04.	BIGO	21:01	12° 21.51'	077° 21.71'	194.4	BIGO deployment
472-1	CTD 61	23.04.	CTD/RO	23:10	12° 13.02'	077° 36.59'	463.9	CTD Station (455m, bottom)
473-1	Trap 2	24.04.	Sediment trap	00:10	12° 12.92'	077° 36.70'	401.8	Recovery drifting sediment trap
474-1	CTD-TM 59	24.04.	CTD-TM	01:44	12° 12.90'	077° 36.74'	404.3	

475-1	CTD 62	24.04.	CTD/RO	02:39	12° 12.96'	077° 36.92'	482.8	CTD Station (460 m)
476-1	ISP 5	24.04.	In-situ pumps	03:36	12° 12.96'	077° 36.92'	481.9	Pumps at 40 m, 100 m, 200 m, 290 m depth
477-1	SC 6	24.04.	Snow catcher	05:52	12° 12.96'	077° 36.92'	480.8	Snow catcher from 70 m depth
478-1	RC 9	24.04.	Rapid Cast	06:11	12° 13.09'	077° 37.03'	507.5	
479-1	MSS 25	24.04.	MSS	08:57	12° 12.84'	077° 10.25'	67.7	
480-1	CTD 63	24.04.	CTD/RO	10:00	12° 13.54'	077° 10.79'	75.5	CTD Station (70 m, bottom)
481-1	MSS 26	24.04.	MSS	11:02	12° 13.82'	077° 12.14'	88.8	
482-1	CTD 64	24.04.	CTD/RO	11:57	12° 15.14'	077° 12.88'	103.9	CTD Station (100 m, bottom)
483-1	MUC 8	24.04.	TV-MUC	12:55	12° 13.52'	077° 10.79'	75.5	Multicorer 74 m
484-1	SML	24.04.	SML	14:30	12° 13.520'	077° 10.790'	75.0	Deployment satellite mini
485-1	POZ	24.04.	POZ	16:35	12° 16.690'	077°14.992'	127.0	Deployment POZ lander
486-1	CTD 65	24.04.	CTD/RO	16:55	12° 16.77'	077° 15.04'	128.3	CTD Station (125 m, bottom)
487-1	CTD-TM 60	24.04.	CTD-TM	19:24	12° 16.77'	077° 15.04'	128.2	
488-1	BIGO II-3	24.04.	BIGO	21:05	12° 16.79'	077° 15.01'	128.1	BIGO deployment
489-1	MSS 27	24.04.	MSS	21:24	12° 16.83'	077° 15.02'	127.9	
490-1	MSS 28	24.04.	MSS	23:22	12° 20.59'	077° 21.35'	181.4	
491-1	CTD 66	25.04.	CTD/RO	00:31	12° 21.52'	077° 21.73'	193.7	CTD Station (190 m, bottom)
492-1	CTD 67	25.04.	CTD/RO	03:04	12° 23.42'	077° 38.09'	575.5	CTD Station (200 m)
493-1	RC 10	25.04.	Rapid Cast	03:33	12° 23.52'	077° 39.05'	636.0	
494-1	CTD 68	25.04.	CTD/RO	07:00	12° 19.39'	078° 10.28'	2539.4	CTD Station (400 m)
495-1	CTD 69	25.04.	CTD/RO	08:11	12° 19.77'	078° 05.25'	2066.5	CTD Station (700 m)
496-1	RC 11	25.04.	Rapid Cast	08:47	12° 19.97'	078° 05.56'	2060.0	
497-1	BIGO I-2	25.04.	BIGO	13:42	12° 21.43'	077° 21.72'	194.1	BIGO recovery
498-1	BWS	25.04.	BWS	15:08	12° 16.69'	077° 14.99'	129.0	Deployment failed
499-1	CTD-TM 61	25.04.	CTD-TM	15:42	12° 16.69'	077° 14.99'	127.1	
500-1	BWS	25.04.	BWS	16:35	12° 16.69'	077° 15.02'	127.1	Deployment failed
501-1	BWS	25.04.	BWS	17:28	12° 16.68'	077° 15.02'	127.8	Deployment failed
502-1	GLI 5	25.04.	GLIDER	19:26	12° 22.53'	077° 22.63'	212.1	Deployment Glider IFM09
503-1	BIGO I-3	25.04.	BIGO	22:11	12° 18.70'	077° 17.79'	143.7	BIGO deployment
504-1	BWS 2	25.04.	BWS	22:56	12° 18.65'	077° 17.78'	143.2	
505-1	CTD 70	25.04.	CTD/RO	23:26	12° 18.65'	077° 17.78'	143.1	CTD Station (140 m, bottom)
506-1	MSS 29	26.04.	MSS	00:23	12° 18.67'	077° 17.79'	143.2	
507-1	MSS 30	26.04.	MSS	03:35	12° 26.05'	077° 29.09'	374.1	
508-1	CTD 71	26.04.	CTD/RO	04:39	12° 27.19'	077° 29.51'	404.9	CTD Station (400 m, bottom)
509-1	MSS 31	26.04.	MSS	05:56	12° 23.88'	077° 26.04'	280.3	
510-1	CTD 72	26.04.	CTD/RO	06:57	12° 24.23'	077° 26.43'	296.0	CTD Station (295 m, bottom)
511-1	MSS 32	26.04.	MSS	08:16	12° 22.96'	077° 23.86'	231.6	
512-1	CTD 73	26.04.	CTD/RO	09:18	12° 23.32'	077° 24.25'	243.4	CTD Station (240 m, bottom)
513-1	BIGO II-3	26.04.	BIGO	13:21	12° 16.78'	077° 15.01'	125.3	BIGO recovery
514-1	RC 12	26.04.	Rapid Cast	14:41	12° 16.33'	077° 24.30'	219.9	
515-1	Trap 4	26.04.	Sediment trap	20:49	12° 19.96'	078° 03.18'	1971.1	Deployment drifting sediment trap
516-1	CTD 74	26.04.	CTD/RO	21:10	12° 20.29'	078° 03.07'	1969.8	CTD Station (730 m)
517-1	CTD-TM 62	26.04.	CTD-TM	22:06	12° 20.29'	078° 03.07'	1971.0	
518-1	MSS 33	27.04.	MSS	00:08	12° 20.38'	078° 03.32'	1988.5	
519-1	ISP 6	27.04.	In-situ pumps	01:21	12° 21.16'	078° 03.39'	2020.6	Pumps at 30 m, 100 m, 200 m, 590 m depth
520-1	CTD 75	27.04.	CTD/RO	04:42	12° 19.98'	077° 58.01'	1716.9	CTD Station (700 m)
521-1	CTD 76	27.04.	CTD/RO	06:05	12° 19.97'	077° 52.00'	1577.1	CTD Station (700 m)
522-1	CTD 77	27.04.	CTD/RO	07:24	12° 20.01'	077° 45.99'	1389.4	CTD Station (700 m)
523-1	CTD 78	27.04.	CTD/RO	08:44	12° 19.99'	077° 39.97'	1054.1	CTD Station (700 m)
524-1	CTD 79	27.04.	CTD/RO	10:03	12° 19.99'	077° 34.00'	381.8	CTD Station (380 m, bottom)
525-1	CTD 80	27.04.	CTD/RO	11:40	12° 23.33'	077° 24.17'	243.6	CTD Station (240 m, bottom)

526-1	BIGO I-3	27.04.	BIGO	13:25	12° 18.59'	077° 17.74'	144.0	BIGO recovery
527-1	SC 7	27.04.	Snow catcher	14:45	12° 23.30'	077° 24.17'	241.8	Snow catcher from 140 m depth
528-1	MSS 34	27.04.	MSS	15:16	12° 23.35'	077° 24.18'	242.7	
529-1	MSS 35	27.04.	MSS	17:54	12° 14.08'	077° 12.68'	94.1	
530-1	CTD 81	27.04.	CTD/RO	18:54	12° 14.67'	077° 12.80'	100.3	CTD Station (90 m, bottom)
531-1	MSS 36	27.04.	MSS	19:42	12° 12.98'	077° 10.67'	69.9	
532-1	CTD 82	27.04.	CTD/RO	20:40	12° 13.50'	077° 10.78'	74.1	CTD Station (70 m, bottom)
533-1	BIGO II-4	27.04.	BIGO	21:17	12° 13.50'	077° 10.78'	73.6	BIGO deployment
534-1	CTD 83	27.04.	CTD/RO	21:55	12° 11.66'	077° 08.37'	41.3	CTD Station (40 m, bottom)
535-1	CTD-TM 63	27.04.	CTD-TM	22:14	12° 11.66'	077° 08.37'	42.0	
536-1	RC 13	27.04.	Rapid Cast	22:35	12° 11.75'	077° 08.44'	44.4	
537-1	MSS 37	27.04.	MSS	23:28	12° 13.19'	077° 11.56'	76.7	
538-1	CTD 84	28.04.	CTD/RO	00:54	12° 14.32'	077° 11.86'	90.6	CTD Station (85 m, bottom)
539-1	MSS 38	28.04.	MSS	02:31	12° 20.26'	077° 21.76'	183.2	
540-1	CTD 85	28.04.	CTD/RO	03:56	12° 21.48'	077° 21.71'	191.9	CTD Station (190 m, bottom)
541-1	MSS 39	28.04.	MSS	05:28	12° 25.19'	077° 29.59'	358.0	
542-1	CTD 86	28.04.	CTD/RO	07:51	12° 25.51'	077° 29.59'	366.9	CTD Station (360 m, bottom)
543-1	MUC 9	28.04.	TV-MUC	13:11	12° 31.35'	077° 35.01'	750.5	Multicorer 750 m
544-1	KPO1182	28.04.	Mooring	17:14	12° 34.732’	077° 39.618’	999.0	Mooring deployment
545-1	BIGO I-4	28.04.	BIGO	18:27	12° 34.88'	077° 40.39'	974.9	BIGO deployment
546-1	RC 14	28.04.	Rapid Cast	18:54	12° 34.95'	077° 40.38'	979.3	
547-1	CTD 87	28.04.	CTD/RO	23:17	12° 32.80'	078° 27.60'	4332.3	CTD Station (600 m)
548-1	Trap 3	29.04.	Sediment trap	00:00	12° 32.78'	078° 27.86'	4357.3	Recovery drifting sediment trap
549-1	CTD 88	29.04.	CTD/RO	01:52	12° 32.84'	078° 28.03'	4358.3	CTD Station (400 m)
550-1	SC 8	29.04.	Snow catcher	02:54	12° 32.84'	078° 28.03	4357.5	Snow catcher closed at 130 m depth
551-1	ISP 7	29.04.	In-situ pumps	03:25	12° 32.84'	078° 28.03'	4354.8	Pumps at 50 m, 100 m, 200 m, 590 m depth
552-1	RC 15	29.04.	Rapid Cast	05:42	12° 32.85'	078° 27.83'	4374.2	
553-1	BIGO II-4	29.04.	BIGO	14:03	12° 13.59'	077° 10.75'	76.0	BIGO Recovery
554-1	CTD 89	29.04.	CTD/RO	14:53	12° 15.09'	077° 12.89'	105.9	CTD Station (100 m, bottom)
555-1	CTD 90	29.04.	CTD/RO	16:35	12° 21.49'	077° 2.71'	194.7	CTD Station (190 m, bottom)
556-1	CTD-TM 64	29.04.	CTD-TM	17:26	12° 21.47'	077° 21.79'	194.9	
557-1	BWS 3	29.04.	BWS	18:22	12° 21.42'	077° 21.91'	194.4	
558-1	GLI 6	29.04.	GLIDER	21:29	12° 34.79'	077° 40.41'	967.0	Deployment Glider IFM03
559-1	CTD 91	29.04.	CTD/RO	22:11	12° 34.84'	077° 40.39'	973.8	CTD Station (970 m, bottom)
560-1	MSS 40	29.04.	MSS	23:56	12° 34.87'	077° 40.40'	973.3	
561-1	CTD-TM 65	30.04.	CTD-TM	11:18	12° 35.03'	077° 40.46'	985.9	
562-1	BIGO I-4	30.04.	BIGO	13:42	12° 34.58'	077° 40.57'	956.3	BIGO recovery
563-1	Trap 4	30.04.	Sediment trap	19:17	12° 16.27'	078° 35.06'	3456.6	Recovery drifting sediment trap
564-1	RC 16	30.04.	Rapid Cast	21:08	12° 16.10'	078° 35.76'	3396.7	
565-1	GLI 7	30.04.	GLIDER	23:28	12° 13.56'	078° 18.75'	2745.6	Recovery Glider IFM12
566-1	RC 17	01.05.	Rapid Cast	00:03	12° 13.56'	078° 19.33'	2775.1	
567-1	CTD 92	01.05.	CTD/RO	01:12	12° 17.13'	078° 30.02'	3188.7	CTD Station (2000 m)
568-1	SC 9	01.05.	Snow catcher	02:52	12° 17.12'	078° 29.95'	3178.9	Snow catcher closed at 230 m depth
569-1	CTD 93	01.05.	CTD/RO	03:40	12° 17.12'	078° 29.95'	3176.4	CTD Station (400 m)
570-1	ISP 8	01.05.	In-situ pumps	04:22	12° 17.13'	078° 29.96'	3180.3	Pumps at 50 m, 100 m, 300 m, 490 m depth
571-1	RC 18	01.05.	Rapid Cast	06:32	12° 16.95'	078° 30.49'	3200.2	
572-1	CTD-TM 66	01.05.	CTD-TM	09:40	12° 18.94'	078° 04.45'	1992.4	
573-1	RC 19	01.05.	Rapid Cast	11:22	12° 18.88'	078° 05.06'	2013.8	

574-1	MUC 10	01.05.	TV-MUC	15:39	12° 24.90'	077° 26.29'	302.4	Multicorer 300 m
575-1	MSS 41	01.05.	MSS	17:24	12° 19.17'	077° 20.44'	165.7	
576-1	CTD 94	01.05.	CTD/RO	18:19	12° 20.12'	077° 20.73'	174.1	CTD Station (170 m, bottom)
577-1	MUC 11	01.05.	TV-MUC	20:09	12° 15.16'	077° 12.88'	105.5	Multicorer 100 m
578-1	GLI 8	01.05.	GLIDER	22:15	12° 23.32'	077° 24.21'	241.7	Deployment Glider IFM13
579-1	CTD 95	01.05.	CTD/RO	22:58	12° 23.49'	077° 24.30'	246.1	CTD Station (240 m, bottom)
580-1	MSS 42	02.05.	MSS	00:33	12° 28.90'	077° 32.61'	506.8	
581-1	CTD 96	02.05.	CTD/RO	01:44	12° 29.91'	077° 32.92'	549.9	CTD Station (550 m, bottom)
582-1	MSS 43	02.05.	MSS	02:59	12° 32.16'	077° 37.47'	912.1	
583-1	CTD 97	02.05.	CTD/RO	04:10	12° 33.14'	077° 37.68'	947.1	CTD Station (940 m, bottom)
584-1	MSS 44	02.05.	MSS	06:14	12° 36.83'	077° 43.66'	1100.2	
585-1	CTD 98	02.05.	CTD/RO	07:12	12° 36.97'	077° 43.82'	1112.2	CTD Station (1110 m,
586-1	MSS 45	02.05.	MSS	08:52	12° 40.49'	077° 48.66'	1615.9	
587-1	CTD 99	02.05.	CTD/RO	10:07	12° 41.14'	077° 48.76'	1692.7	CTD Station (1700 m,
588-1	MUC 12	02.05.	TV-MUC	13:02	12° 34.90'	077° 40.34'	979.3	Multicorer 1000 m
589-1	CTD-TM 67	02.05.	CTD-TM	15:24	12° 27.20'	077° 29.55'	406.5	
590-1	OFOS 1	02.05.	OFOS	16:59	12° 26.10'	077° 27.93'	350.7	
591-1	OFOS 2	02.05.	OFOS	18:29	12° 24.90'	077° 26.37'	305.0	
592-1	OFOS 3	02.05.	OFOS	19:55	12° 23.29'	077° 24.18'	241.1	
593-1	OFOS 4	02.05.	OFOS	21:16	12° 21.48'	077° 21.70'	194.7	

7.2 Station list of marine gel particle samples

METEOR	Latitude	Longitude	Pigments	Particulate organic carbon	Transparent exopolymer particles for microscopy	Coomassie stainable particles for microscopy	Partuiclulate organic Phosphorus (POP)
Station	°S	°W	sampling depth (m)	sampling depth (m)	sampling depth (m)	sampling depth (m)	sampling depth (m)
339	13° 54.39’	076°20.67'	5, 11, 16, 20, 30, 40, 50, 70, 100, 130, 160	5, 20, 50, 100	5, 20, 50, 100	-	-
358	14° 10.92’	076°55.86’	5, 15, 30, 50, 80, 100, 125, 200, 400, 600, 1995	5, 50, 200, 600	5, 50, 200, 600	-	-
368	14°28.14’	077°21.24’	5, 50, 90, 100, 150, 200, 300, 400, 500, 600, 2000	5, 50, 90, 100, 150, 200, 300, 400, 500, 600, 2000	5, 50, 90, 100, 150, 200, 300, 400, 500, 600	5, 50, 90, 100, 150, 200, 300, 400, 500, 600	5, 50, 90, 100, 150, 200, 300, 400, 500, 600
380	15°21.63’	077°09.89’	5, 20, 30, 65, 100, 120, 150, 200, 400, 600	5, 20, 30, 65, 100, 120, 150, 200, 400, 600	5, 30, 100, 150	-	-
393	15°21.00’	076°55.80’	5, 20, 40, 60, 100, 110, 130, 150, 200, 300, 400	5, 20, 40, 60, 100, 110, 130, 150, 200, 300, 400	5, 60, 110, 200	-	-
402	14°34.50’	077°16.24’	5, 50, 100, 150, 200, 300, 400, 500, 600	5, 50, 100, 150, 200, 300, 400, 500, 600	5, 50, 100, 150, 200, 300, 400, 500, 600	5, 50, 100, 150, 200, 300, 400, 500, 600	5, 50, 100, 150, 200, 300, 400, 500, 600
432	12°18.00'	077°36.95'	5, 10, 40, 100, 150, 200, 300	5, 10, 40, 100, 150, 200, 300	5, 10, 40, 100, 150, 200, 300	5, 10, 40, 100, 150, 200, 300	5, 10, 40, 100, 150, 200, 300
446	12°31.36’	077°35.00'	5, 30, 40, 50, 60, 80, 90, 100, 150, 600, 746	30, 50, 100, 600	30, 50, 100, 600	-	-
457	12°24.90’	077°26.30'	5, 20, 51, 100, 125, 150, 175, 225, 275, ~300	5, 20, 51, 100, 125, 150, 175, 225, 275, ~300	5, 20, 51, 100, 125, 150, 175, 225, 275, ~300	5, 20, 51, 100, 125, 150, 175, 225, 275, ~300	-
459	12°27.21’	077°29.52'	-	30, 80, 150, 300	-	-	-
467	12°59.25’	078°14.82’	10, 50, 75, 100, 200, 300, 400, 500, 600	10, 50, 75, 100, 200, 300, 400, 500, 600	10, 50, 75, 100, 200, 300, 400, 500, 600	10, 50, 75, 100, 200, 300, 400, 500, 600	10, 50, 75, 100, 200, 300, 400, 500, 600
472	12°12.91'	077°36.66’	5, 40, 100, 150, 200, 300	5, 40, 100, 150, 200, 300	5, 40, 100, 150, 200, 300	5, 40, 100, 150, 200, 300	5, 40, 100, 150, 200, 300
495	12° 19.77'	078° 05.25'	30, 75, 100, 150, 200, 400	30, 75, 100, 150, 200, 400	-	-	-
508	12°27.21'	077°29.52'	5, 20, 30, 60, 100, 200, 300	5, 30, 60, 100	5, 30, 60, 100	-	-
516	12°20.00‘	077°58.00'	10, 50, 100, 150, 200, 300, 400, 500, 600	10, 50, 100, 150, 200, 300, 400, 500 600	10, 50, 100, 150, 200, 300, 400, 500, 600	10, 50, 100, 150, 200, 300, 400, 500, 600	10, 50, 100, 150, 200, 300, 400, 500, 600
532	12°13.51'	077°10.79'	5, 20, 30, 40, 60, 75	5, 20, 30, 40, 60, 75	5, 20, 30, 40, 60, 75	-	-
547	12°32.80'	078°27.50'	10, 50, 75, 100, 200, 300, 400, 500, 600	10, 50, 75, 100, 200, 300, 400, 500, 600	10, 50, 75, 100, 200, 300, 400, 500, 600	10, 50, 75, 100, 200, 300, 400, 500, 600	10, 50, 75, 100, 200, 300, 400, 500, 600
559	12°34.91'	077°40.37'	5, 30, 50, 70, 100, 200, 600	5, 30, 70, 100, 600	5, 30, 70, 100, 200, 600	-	-
566	12°17.12’	078°29.89’	5, 50, 100, 150, 200, 300, 400, 500, 600	5, 50, 100, 150, 200, 300, 400, 500, 600	5, 50, 100, 150, 200, 300, 400, 500, 600	5, 50, 100, 150, 200, 300, 400, 500, 600	5, 50, 100, 150, 200, 300, 400, 500, 600

METEOR	Latitude	Longitude	Transparent exopolymer particles for colorimetric method	Transparent exopolymer particles for colorimetric method	Biogenic silica (BSi)	Particulate hydrolysable amino acids	Particulate carbohydrates
station	°S	°W	sampling depth (m)	sampling depth (m)	sampling depth (m)	sampling depth (m)	sampling depth (m)
339	13°54.39'	076°20.67'	-	-	-	-	-
358	14°10.92’	076°55.86’	-	-	-	-	-
368	14°28.14’	077°21.24’	5, 50, 90, 100, 150, 200, 300, 400, 500, 600	5, 50, 90, 100, 150, 200, 300, 400, 500, 600	5, 50, 90, 100, 150, 200, 300, 400, 500, 600	-	-
380	15°21.63’	077°09.89’	-	-	-	-	-
393	15°21.00’	076°55.80’	-	-	-	-	-
402	14°34.50’	077°16.24’	-	-	5, 50, 100, 150, 200, 300, 400, 500, 600	-	-
432	12°18.00'	077°36.95'	-	-	5, 10, 40, 100, 150, 200, 300	5, 10, 40, 100, 150, 200, 300	5, 10, 40, 100, 150, 200, 300
446	12°31.36’	077°35.00'	-	-	-	-	-
457	12°24.90’	077°26.30'	-	-	-	-	-
459	12°27.21’	077°29.52'	-	-	-	-	-
467	12°59.25’	078°14.82’	-	-	10, 50, 75, 100, 200, 300, 400, 500, 600	10, 50, 75, 100, 200, 300, 400, 500, 600	10, 50, 75, 100, 200, 300, 400, 500, 600
472	12°12.91'	077°36.66'	-	-	5, 40, 100, 150, 200, 300	5, 40, 100, 150, 200, 300	5, 40, 100, 150, 200, 300
495			-	-	-	-	-
508	12°27.21'	077°29.52'	-	-	-	-	-
516	12°20.00‘	077°58.00'	10, 50, 100, 150, 200, 300, 400, 500, 600	10, 50, 100, 150, 200, 300, 400, 500, 600	10, 50, 100, 150, 200, 300, 400, 500, 600	10, 50, 100, 150, 200, 300, 400, 500 600	10, 50, 100, 150, 200, 300, 400, 500 600
532	12°13.51'	077°10.79'	-	-	-	-	-
547	12°32.80'	078°27.50'	-	-	10, 50, 75, 100, 200, 300, 400, 500, 600	10, 50, 75, 100, 200, 300, 400, 500, 600	10, 50, 75, 100, 200, 300, 400, 500, 600
559	12°34.91'	077°40.37'	-	-	-	-	-
566	12°17.12’	078°29.89’	-	-	5, 50, 100, 150, 200, 300, 400, 500, 600	5, 50, 100, 150, 200, 300, 400, 500, 600	5, 50, 100, 150, 200, 300, 400, 500, 600

8 Data and sample storage and availability

In Kiel, a joint data management team is set up to store the data from various projects and cruises in a web-based multi-user-system. Data gathered during M136 are stored at the Kiel data portal OSIS, and remain proprietary for the PIs of the cruise and for members of SFB 754 project. All data will be submitted to PANGAEA within 3 years after the cruise, i.e. latest by June 2020. Some of the data sets collected during M136 have already been made publically available. Digital object identifiers (DOIs) are automatically assigned to data sets archived in the PANGAEA Open Access library making them publically retrievable, citeable and reusable for the future. All metadata are publically available via the following link pointing at the GEOMAR portal https://portal.geomar.de/metadata/leg/show/341102.

Preliminary CTD data were submitted to CORIOLIS during the cruise for real time oceanographic analysis and Argo calibration. Contact persons for the different datasets are listed in Table 8.1 below.

Table 8.1 Overview of data availability. Data will be available one year after the cruise on the Kiel Ocean Data Information Centre (OSIS). Here, data description but not the data itself is publically available. After three years or earlier, data will be made publically available on the World Data Center PANGAEA. Links to published data are marked in blue.

Type	Database	Available	Free Access doi.pangaea.de/10.1594/	Contact Person
CTD/O_2 - profiles	PANGAEA	May 2018	PANGAEA.904013,	Gerd Krahmann, GEOMAR, gkrahmann@geomar.de
Microstructure shear and temperature profiles	PANGAEA	May 2018	PANGAEA.890121	Marcus Dengler, GEOMAR, mdengler@geomar.de
ADCP, 38kHz and 75kHz	PANGAEA	May 2019	PANGAEA.901425	Marcus Dengler, GEOMAR, mdengler@geomar.de
Underway Thermosalinograph data	PANGAEA	June 2019	PANGAEA.904288	Gerd Krahmann, GEOMAR, gkrahmann@geomar.de
Glider data (T, S, P, O_2, chl-*a*, turb., NO_3, microstructure)	PANGAEA	Apr. 2018 (OSIS)	June 2020	Gerd Krahmann, GEOMAR, gkrahmann@geomar.de
Hydrochemistry of water samples (O_2, nutrients)	PANGAEA	Oct. 2019	PANGAEA.904404	Stefan Sommer, GEOMAR ssommer@geomar.de
In situ benthic nutrient and oxygen fluxes	PANGAEA	Apr. 2018 (OSIS)	June 2020	Stefan Sommer, GEOMAR ssommer@geomar.de
Bacterial Biomass Production, Extracellular Enzyme Rates, Bacterial Cell Abundances, DOC, DON water column	PANGAEA	Oct. 2019	PANGAEA.891247	Anja Engel, GEOMAR, aengel@geomar.de
Trace metals (dissolved and particles), Fe(II), pH, TOC, Fe-L.	PANGAEA	Dec. 2018 (OSIS)	June 2020	Eric Achterberg, GEOMAR eachterberg@geomar.de
DOP, DON, nutrients from Trace Metal CTD	PANGAEA	Dec. 2018 (OSIS)	June 2020	Eric Achterberg, GEOMAR eachterberg@geomar.de
Cd isotopes, dissolved ^{238}U and total ^{234}Th	PANGAEA	Dec. 2018 (OSIS)	June 2020	Eric Achterberg, GEOMAR eachterberg@geomar.de
Porewater data and experiments (NH_4, PO_4, Fe, H_2S, DIC, DOC, C/N ratio, Por.)	PANGAEA	Apr. 2018 (OSIS)	June 2020	Andy Dale, GEOMAR, adale@geomar.de
$\Delta^{15}N$, $\Delta^{13}C$, NO_3 NO_2 isotopes, N & C fixation rates, N reduction rates, N_2, N_2O, DNRA, NH_4 oxidation, N/Ar ratio, PP.	PANGAEA	Apr. 2018 (OSIS)	June 2020	Gaute Lavik, MPI Bremen glavik@mpi-bremen.de
Sediment trap data: POC, PON, POP, DSi-bio, Amino Acids, Carbohydrates, particles, TEP, DNA, Coomassie.	PANGAEA	Apr. 2018 (OSIS)	June 2020	Anja Engel, GEOMAR, aengel@geomar.de
UVP data (number and sizes of particle, Zooplankton)	PANGAEA	Apr. 2018 (OSIS)	June 2020	Rainer Kiko, GEOMAR, rkiko@geomar.de
Underway surface N_2O, CO, CO_2 concentrations.	PANGAEA	Apr. 2018 (OSIS)	June 2020	Damian Arévalo-Martínez darevalo@geomar.de
Viral community analysis (DNA, RNA), Microbial community analysis	PANGAEA	Apr. 2018 (OSIS)	June 2020	Martin Fischer, Uni Kiel mfischer@ifam.uni-kiel.de

9 Acknowledgements

We are grateful to Capitan Schubert and his crew for the excellent collaboration and the pleasant working atmosphere during the cruise. The crew of FS METEOR greatly contributed to the success of the cruise. We also acknowledge the support of the Peruvian Ministerio De La Producción and the German Ministry of Foreign Affairs for the allowance to conduct research in

Peruvian waters. Additionally, we express our gratitude to the Leitstelle METEOR/MERIAN for its valuable support. The ship time of METEOR was provided by the German Science Foundation (DFG) within the core program METEOR/MERIAN. Financial support was provided by the German Science Foundation (DFG) as part of the SFB754 "Climate Biogeochemistry Interactions in the Tropical Ocean".

10 References

Bohlen, L., Dale, A. W., Sommer, S., Mosch, T., Hensen, C., Noffke, A., Scholz, F., Wallmann, K., 2011. Benthic nitrogen cycling traversing the Peruvian oxygen minimum zone. Geochimica et Cosmochimica Acta 75, 6094-6111.

Brandt, P., Bange, H.W., Banyte, D., Dengler, M., Didwischus S.H., Fischer, T., Greatbatch, R. J., Hahn, J., Kanzow, T., Karstensen, J., Körzinger, A., Krahmann, G., Schmidtko, S., Tanhua, T., Visbeck, M., 2015. On the role of circulation and mixing in the ventilation of oxygen minimum zones with a focus on the eastern tropical North Atlantic. *Biogeosciences*, 12, 489-512.

Chaigneau, A., Dominguez, N., Eldin, G., Vasquez, L., Flores, R., Grados, C., Echevin, V., 2013. Near-coastal circulation in the Northern Humboldt Current System from shipboard ADCP data. *J. Geophys. Res. Oceans*, 118, 5251-5266. doi:10.1002/jgrc.20328.

Cisternas Novoa, C., Lee, C., Engel, A., 2015. Transparent exopolymer particles (TEP) and Coomassie stainable particles (CSP): Differences between their origin and vertical distributions in the ocean. *Marine Chemistry*, 175, 56-71.

Dale, A.W., Sommer S., Lomnitz, U., Bourbonnais, A., Wallmann, K., 2016. Biological nitrate transport in sediments on the Peruvian margin mitigates benthic sulfide emissions and drives pelagic N loss during stagnation events. *Deep. Res. I*, 112, 123–136.

Engel, A., Wagner, H., Le Moigne, F.A.C. and Wilson, S.T., 2017. Particle export fluxes to the oxygen minimum zone of the Eastern Tropical North Atlantic. *Biogeosciences*, 14, 1825-1838.

Engel, A., Galgani, L., 2016. The organic sea-surface microlayer in the upwelling region off the coast of Peru and potential implications for air-sea exchange processes. *Biogeosciences* 13, 989–1007.

Engel, A., Händel, N., 2011. A novel protocol for determining the concentration and composition of sugars in particulate and in high molecular weight dissolved organic matter (HMW-DOM) in seawater. *Mar. Chem.*, 127, 180–191.

Erdem, Z., Schönfeld, J., Glock, N., Dengler, M., Mosch, T., Sommer, S., Elger, J., Eisenhauer, A., 2016 .Peruvian sediments as recorders of an evolving hiatus for the last 22 thousand years. *Quaternary Science Reviews*, 137, 1-14.

Fuenzalida, R., Schneider, W., Garcés, J., Bravo, L. and Lange, C., 2009. Vertical and horizontal extension of the oxygen minimum zone in the eastern South Pacific Ocean. *Deep-Sea Res. II*, 56, 992-1003, doi:10.1016/j.dsr2.2008.11.001.

Gasol, J. M., Del Giorgio, P. A., 2000. Using flow cytometry for counting natural planktonic bacteria and understanding the structure of planktonic bacterial communities. *Sci. Mar.*, 64, 197–224.

Grasshoff, K., Kremlin, K., Ehrhardt, M., 1999. Methods of seawater analysis. 3rd ed., eds. K. Grasshoff, K. Kremlin, and M. Ehrhardt Weinheim: Wiley-VCH, Weinheim.

Gutiérrez, D., Enríquez, E., Purca, S., Quipúzcoa, L., Marquina, R., Flores, G., Graco, M., 2008. Oxygenation episodes on the continental shelf of central Peru: Remote forcing and benthic ecosystem response. *Prog. Oceanogr.* 79, 177–189.

Hoppe, H. G., 1983. Significance of exoenzymatic activities in the ecology of brackish water: measurements by means of methylumbelliferyl-substrates. *Mar. Ecol. Prog. Ser.*, 11, 299–308.

Kalvelage, T. et al., 2013. Nitrogen cycling driven by organic matter export in the South Pacific oxygen minimum zone. *Nature Geoscience*, 6, 228-234.

Kirchman, D., K'nees, E., Hodson, R., 1985. Leucine incorporation and its potential as a measure of protein synthesis by bacteria in natural aquatic systems. Appl. *Environm. Microbiol*. 49, 599–607.

Knauer, G.A., Martin, J.H., Bruland, K.W., 1979. Fluxes of particulate carbon, nitrogen, and phosphorus in the upper water column of the northeast Pacific. *Deep-Sea Research*, 26, 97-108.

Laurenceau-Cornec, E.C., et al., 2015. The relative importance of phytoplankton aggregates and zooplankton fecal pellets to carbon export: insights from free-drifting sediment trap deployments in naturally iron-fertilised waters near the Kerguelen Plateau. *Biogeosciences*, 12, 1007-1027.

Lindroth, P., Mopper, K., 1979. High performance liquid chromatographic determination of subpicomole amounts of amino acids by precolumn fluorescence derivatization with o-phthaldialdehyde. *Anal. Chem.*, 51, 1667–1674.

Marshall, D. P., Tansley, C. E., 2001. An implicit formula for boundary current separation. *J. Phys. Oceanogr.*, 31, 6, 1633–1638.

Mosch, T., Sommer, S., Dengler, M., Noffke, A., Bohlen, L., Pfannkuche, O., Liebetrau, V., Wallmann, K., 2012. Factors influencing the distribution of epibenthic megafauna across the Peruvian oxygen minimum zone. *Deep-Sea Res. I*, 68, 123-135.

Nausch, M., Nausch, G., 2000. Stimulation of peptidase activity in nutrient gradients in the Baltic Sea. Soil Biol. *Biochem.*, 32, 1973–1983.

Pantoja, S., Rossel, P., Castro, R., Cuevas, L. A., Daneri, G., Córdovan, C., 2009. Microbial degradation rates of small peptides and amino acids in the oxygen minimum zone of Chilean coastal waters. *Deep. Res. II Trop. Stud. Oceanogr.*, 56, 1055–1062.

Pietri, A., Echevin, V., Testor, P., Chaigneau, A., Mortier, L., Grados, C., and Albert, A., 2014. Impact of a coastal-trapped wave on the near-coastal circulation of the Peru upwelling system from glider data, *J. Geophys. Res. Oceans*, 119, 2109-2120.

Pike, S., Buesseler, K., Andrews, J., Savoye, N., 2005. Quantification of 234Th recovery in small volume sea water samples by inductively coupled plasma-mass spectrometry. *Journal of Radioanalytical and Nuclear Chemistry*, 263, 355-360.

Rapp, I., Schlosser, C., Rusiecka, D., Gledhill, M., Achterberg, E.P. 2017. Automated preconcentration of Fe, Zn, Cu, Ni, Cd, Pb, Co, and Mn in seawater with analysis using high-resolution sector field inductively-coupled plasma mass spectrometry. *Analytica Chimica Acta*, 976, 1-13.

Sommer, S., Linke, P., Pfannkuche, O., Schleicher, T., Deimling, J., Schneider, V., Reitz, A., Haeckel, M., Flögel, S., Hensen, C., 2009. Seabed methane emissions and the habitat of

frenulate tubeworms on the captain Arutyunov mud volcano (Gulf of Cadiz). *Mar. Ecol. Prog. Ser.*, 382, 69–86.

Sommer, S., Gier, J., Treude, T., Lomnitz, U., Dengler, M., Cardich, J., Dale, A.W., 2016. Depletion of oxygen, nitrate and nitrite in the Peruvian oxygen minimum zone cause an imbalance of benthic nitrogen fluxes. *Deep-Sea Res I*, 112, 113-122.

Sommer S., Clemens, D., Yücel M., Pfannkuche O., Hall, P.O.J., Almroth-Rosell, E., Schulz-Vogt, H.N., Dale, A.W., 2017. Major bottom water ventilation events do not significantly reduce basin-wide benthic and N and P release in the Eastern Gotland Basin (Baltic Sea). *Front. Mar. Sci*., 4, 18.

Sommer, S., Dengler, M., et al., 2019. Benthic element cycling, fluxes and transport of nutrients and trace metals across the benthic boundary layer in the Peruvian oxygen minimum zone (SFB 754), Cruise No. 137, 06.05. - 29.05.2017, Callao (Peru) – Callao., doi: /doi.org/10.2312/cr_m137.

Sugimura, Y., Suzuki, Y., 1988. A high-temperature catalytic oxidation method for the determination of non-volatile dissolved organic carbon in seawater by direct injection of a liquid sample. *Mar. Chem.*, 24, 105–131.

Thomsen, S., Kanzow, T., Krahmann, G., Greatbatch, R.J., Dengler, M., Lavik, G., 2016. The formation of a subsurface anticyclonic eddy in the Peru-Chile Undercurrent and its impact on the near-coastal salinity, oxygen, and nutrient distributions *J. Geophys. Res. Oceans*, 121, 476-501.

Torriani, A., 1960. Influence of inorganic phosphate in the formation of phosphatases by Escherichia coli. *Biochim. Biophys. Acta*, 38, 460–469.

Visbeck et al., Cruise No. 135, 01.03. - 08.04.2017, Callao (Peru) - Callao, submitted.